

2018

Synthesis of aromatic dicarboxylates and unique approaches to automated synthesis

Zachary Benjamin Weinstein
Iowa State University

Follow this and additional works at: <https://lib.dr.iastate.edu/etd>

 Part of the [Organic Chemistry Commons](#)

Recommended Citation

Weinstein, Zachary Benjamin, "Synthesis of aromatic dicarboxylates and unique approaches to automated synthesis" (2018). *Graduate Theses and Dissertations*. 17355.
<https://lib.dr.iastate.edu/etd/17355>

This Dissertation is brought to you for free and open access by the Iowa State University Capstones, Theses and Dissertations at Iowa State University Digital Repository. It has been accepted for inclusion in Graduate Theses and Dissertations by an authorized administrator of Iowa State University Digital Repository. For more information, please contact digirep@iastate.edu.

Synthesis of aromatic dicarboxylates and unique approaches to automated synthesis

by

Zachary Benjamin Weinstein

A dissertation submitted to the graduate faculty

in partial fulfillment of the requirements for the degree of

DOCTOR OF PHILOSOPHY

Major: Organic Chemistry

Program of Study Committee:

Aaron D. Sadow, Major Professor

Marek Pruski

Levi Stanley

Javier Vela

Arthur H. Winter

The student author, whose presentation of the scholarship herein was approved by the program of study committee, is solely responsible for the content of this dissertation. The Graduate College will ensure this dissertation is globally accessible and will not permit alterations after a degree is conferred.

Iowa State University

Ames, Iowa

2018

Copyright © Zachary Benjamin Weinstein, 2018. All rights reserved.

To my grandfather Arnold Stern and my friend Adar Ross

TABLE OF CONTENTS

	Page
ACKNOWLEDGEMENTS	v
ABSTRACT	vii
CHAPTER 1. INTRODUCTION	1
General Introduction	1
Thesis Organization	5
References	5
CHAPTER 2. SYNTHESIS AROMATIC DICARBOXYLIC ACIDS VIA CATALYTIC DISPROPORTIONATION WITH COPPER(I) IODIDE	
Abstract	10
Introduction	10
Results and Discussion	15
Conclusion	25
Experimental	26
References	29
CHAPTER 3. UNIQUE APPROACHES TO CATALYSIS ON AN AUTOMATED SYNTHESIS PLATFORM	
Abstract	32
General Introduction	33
Introduction: Chemical Kinetics	34
Results and Discussion: Chemical Kinetics	36
Introduction: Heterogeneous Catalysis Synthesis	45
Results and Discussion: Heterogeneous Catalysis Synthesis	47
Introduction: Enyne Metathesis	52

Results and Discussion: Enyne Metathesis	53
Conclusion	55
Experimental	57
References	58
Supporting Information	62
CHAPTER 4. INVESTIGATION OF [XANTPHOSRH(COD)]BARF FOR CATALYTIC REDUCTION OF SECONDARY AND TERTIARY AMIDES BY PHENYLSILANE	
Abstract	65
Introduction	65
Results and Discussion	67
Conclusion	76
Experimental	77
References	78
Supporting Information	81
CHAPTER 5. CONCLUSION	
General Conclusions	100

ACKNOWLEDGEMENTS

I would like to thank my advisor, Prof. Aaron D. Sadow for taking a chance on me, giving me guidance and funding throughout my journey through graduate school and getting me to the point where I can start my career. Thank you to each of my POS committee members, Dr. Jason Chen, Dr. Marek Pruski, Dr. Levi Stanley, Dr. Javier Vela and Dr. Arthur H. Winter for additional guidance, support and taking the time to sit through my talks and give me valuable feedback.

Thank you to all my past and present lab mates in the Sadow group, those who mentored me, those who I have mentored, we've had fun times, meh times and difficult times trudging towards the same goal. We've all been connected through a uniquely special bond. Thank you to all my collaborators at ISU, especially the fruitful collaborations I've had with the Slowing group. Thank you to all the Iowa State support staff, especially Sarah who's been helpful in more ways than just helping me solve NMRs, she's a great matchmaker.

Thank you to all my friends at the poker game, past and present. Special thanks to Mark, Dave and Paul for practically recruiting me to ISU despite my inability to throw a frisbee (or any sort of sporting object). Without having Saturday nights to unwind, this would have been a much more daunting experience. Thank you to my Ames family, Jesse, Sami, Thea and Eli for giving me big picture advice on being a chemist, hoppy beers and dinner feasts that begin at 3 PM and end asleep on a couch before the sun goes down. Zack, Morgan and Silas for the respite from chemistry talk, concerts and feeding me when Sarah is out of town.

Thank you to my loving ex-girlfriend and current wife Sarah for being here for

me throughout this arduous process, and not getting upset when I come home irritable, late at night on a regular basis. In the 6 years you've been in Ames, I've bought 2 loaves of bread and 0 pizzas. Thank you to my family for getting me through well over a decade of university with minimal debt, and not asking me "When are you graduating?" (too many times). Thank you Dr. Bill Odenkirk for showing what can be achieved with proper training in Organometallic Chemistry.

ABSTRACT

The research presented and discussed in this dissertation involves the synthesis of aromatic dicarboxylates via catalytic isomerization or disproportionation, the synthesis of amines via catalytic hydrosilylation of amides and the development of new methods and approaches for studying catalytic reactions on an automated synthesis platform. The automated synthesis platform was utilized for studying kinetics of oxidation reactions of cyclohexane, as well as the synthesis of small molecules in specialized reactors and scalable quantities of heterogeneous catalysts.

Aromatic dicarboxylic acids such as terephthalic acid or 2,5-furandicarboxylic acid can be prepared through catalytic disproportionation or isomerization of their respective metal carboxylate precursors. Copper(I) iodide catalyzes the disproportionation of potassium furoate to 2,5-furandicarboxylate in up to 85% yield at temperatures of 280 – 300 °C under a carbon dioxide rich atmosphere (40 bar). CuI also catalyzes the disproportionation of potassium benzoate to terephthalate in up to 60% yield at temperatures of 320 – 350 °C under carbon dioxide (40 bar).

XantphosRh(cod)BAR^F (cod = 1,5-cyclooctadiene; BAR^F = Tetrakis[3,5-bis(trifluoromethyl)phenyl]borate) was demonstrated to be an excellent catalyst for the reduction of secondary and tertiary amides to secondary and tertiary amines by phenylsilane. Most substrates could be converted at mild temperatures (25 – 60 °C) within 1 h. Tertiary amides required 2 equiv. of PhSiH₃ for full conversion. Secondary amides exhibited side reactions involving disproportionation of N-R and N-H bonds. These side reactions were inhibited by the addition of 10 equiv. of PhSiH₃.

An automated synthesis robot (Chemspeed SWING-XL) was used to prepare surface supported catalysts of Pd on CeO₂, SiO₂, TiO₂ for hydrogenation reactions. These materials were prepared by iterative additions of a dilute pre-catalyst solution followed by slow evaporation of solvent. These materials were used as catalysts for hydrogenolysis experiments, affording cyclohexanol from guaiacol. This instrument was also used to study the kinetics of cyclohexane oxidation reactions catalyzed by a series [tris(oxazoliny)borato]cobalt compounds previously reported in our group. Finally, this same instrument was used to prepare synthetically challenging diene compounds, by slowly adding catalyst to a heated, pressurized reactor using high-pressure peristaltic pumps.

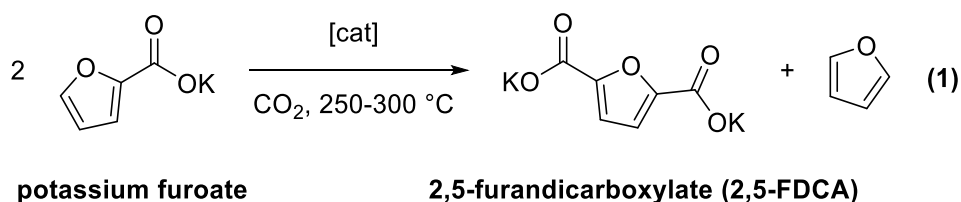
CHAPTER 1. INTRODUCTION

General Introduction

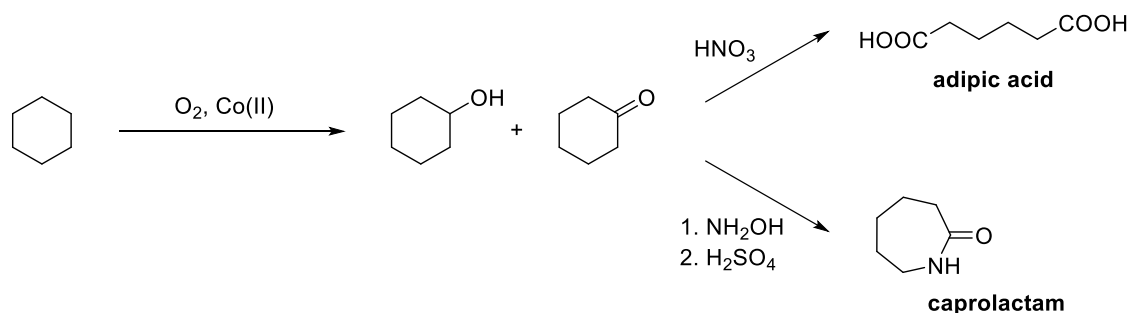
As the global population continues to increase, there is a constantly growing demand for energy, medicine and new materials. To account for growing demand and depleting supplies, development of less energy intensive reactions using sustainable practices, and development of new methods for producing energy from renewable sources is paramount.¹ In fact, many of these needs are currently being sought in part through the synthesis of bio-ethanol from biomass,² bio-diesel from algae,³ organic photovoltaics,⁴ and the use of more abundant metals for catalysis over more precious rare earth metal catalysts.⁵ To achieve these grand, over-arching goals we seek strategies to make iterative changes to improve specific reactions and develop methods to facilitate new, unique or challenging chemistry.

Aromatic dicarboxylates or dicarboxylic acids are commonly used as substrates for polymerization reactions in the production of polyesters. Global demand for polyesters is constantly increasing in the form of fabric, films and packaging materials. Often, these dicarboxylic acid materials such as terephthalic acid (TPA) is prepared through harsh oxidative processes (Amoco Process).^{6,7} Other dicarboxylic acids such as 2,5-furandicarboxylic acid (2,5-FDCA) are prepared using similar processes.⁸⁻¹⁰ The classical method of accessing these materials from a non-oxidative pathway utilizes cadmium salts to catalyze the disproportionation of potassium carboxylates and isomerization of dipotassium dicarboxylates into isomeric dicarboxylates (Henkel Process).¹¹⁻¹⁹ Similar experiments have been performed on heteroaromatic carboxylates to make the dicarboxylate compound 2,5-FDCA (Eq. 1).²⁰⁻²² Innovative catalytic

reactions are required to improve selectivity, yield and avoid cadmium catalysts in favor of more environmentally friendly catalysts. Copper (CuCl_2) has been investigated as a catalyst but was not effective at synthesizing 2,5-FDCA in reasonable yield.²¹ Herein we demonstrate that Cu(I) iodide can be significantly more efficient than even Cd or Zn compounds as catalysts for the synthesis of 2,5-FDCA under high pressures of carbon dioxide at elevated temperatures.



Technological improvements in the field of automation allow for rapid progress in advancing the discovery and optimization of chemical reactions. Strategies such as Design of Experiment (DOE) combined with automation allows for rapid investigation of a broad chemical landscape.²³⁻²⁹ Studying chemical kinetics allows for a more thorough understand of a reaction mechanism. We began to use our synthesis robot to study the kinetics of transition metal catalyzed oxidation reactions of cyclohexane. Selective oxidation of cyclohexane can be challenging,³⁰ but cyclohexanol and cyclohexanone are important precursors for the synthesis of nylon (Scheme 1).³¹

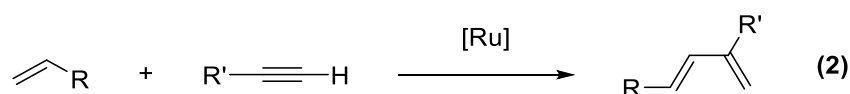


Scheme 1. Conversion of Cyclohexane to Adipic Acid or Caprolactam

Heterogeneous catalysts are used extensively across a broad range of chemical transformations. One strategy for accessing a new source of renewable energy would involve biomass upgrading. Reports of utilizing heterogeneous catalysts to access these kinds of transformations are ubiquitous.^{32–35} Synthesis of heterogeneous catalysis typically involves tedious mixing and grinding of pre-catalyst solutions with the solid support material. Making large libraries of materials can be time consuming and difficult to reproduce accurately. We proposed a method for making a library of materials automatically using a modified variant of “wet impregnation” involving iterative additions of a dilute solution. Iterative addition strategies already exist but involve sputtering of very thin layers of catalyst.³⁶ This method is excellent for preparing a library for primary screening but does not allow for scaling catalyst preparation. These catalysts can be prepared on gram scales and tested in catalytic reactions to assess their potential in a series of hydrogenolysis reactions on lignin model compounds.

Functionalized polymers, macromolecules which are chemically bound to an external functional group, are utilized for making polymers with improved activity or cross-linked polymers, among other uses. Enyne metathesis (Eq. 2) is a potential route for

the synthesis of butadiene derivatives³⁷⁻³⁹ which could be incorporated into polymers, to achieve functionalization without the need to rely on end chain functionalization. These reactions are difficult to optimize in traditional Schlenk-type flasks. Some of the keys to extending the activity of the catalyst include slow catalyst addition and high pressures of ethylene. Using high end instrumentation such as a synthesis robot allows for special consideration of reaction pressure and catalyst addition. Stainless-steel reactors allow for higher pressures of ethylene than pressures traditionally accessed by glass vessels. High-pressure pumps allow the catalyst solution to be added slowly while the reaction is already in progress extending the catalyst lifetime and turnovers.



A common method of accessing amines in the total synthesis of complex molecules is through the reduction of amides.⁴⁰⁻⁴² The conventional method for reducing amides involves reactions with harsh reductants such as lithium aluminum hydride.⁴³ These reductants can be difficult to work with, being sensitive to air and water, and react to give large amounts of salt waste byproducts.⁴⁴⁻⁴⁶ Establishment of late metal catalysts for these reductions are becoming more prevalent. Often these catalysts are only able to reduce either secondary or tertiary amides. We present a cationic Rh-based catalyst which can synthesize a series of both secondary and tertiary amines from their respective amides.

Thesis Organization

This thesis contains four chapters. Chapter 1 provides a general introduction to dicarboxylate isomerization reactions, amide reductions and high-throughput experimentation. Chapter 2, 3 and 4 consists of work that is not yet published, and thus are manuscripts in preparation for publication.

Chapter 2 describes the disproportionation of aromatic carboxylates such as benzoate and furoate to dicarboxylates catalyzed by copper(I) iodide.

Chapter 3 describes our groups approaches towards unique experiments applied on our automated synthesis platform. The first in which we monitor the kinetics of catalytic oxidation reactions, the second in which we prepare and test heterogeneous catalysts, and finally experiments to help optimize enyne metathesis experiments.

Chapter 4 describes the catalytic reduction of tertiary and secondary amines using hydrosilanes catalyzed by a cationic rhodium complex and the study of that complex with hydrosilanes.

Chapter 5 presents general conclusions.

References

- (1) Vogel, G. H. *Chem. Eng. Technol.* **2008**, *31* (5), 730–735.
- (2) Gupta, A.; Verma, J. P. *Renew. Sustain. Energy Rev.* **2015**, *41*, 550–567.
- (3) Demirbas, A. *Appl. Energy* **2011**, *88* (10), 3541–3547.
- (4) Mazzi, K. A.; Luscombe, C. K. *Chem. Soc. Rev.* **2015**, *44* (1), 78–90.

- (5) Zhang, Q.; Kang, J.; Wang, Y. *ChemCatChem* **2010**, 2 (9), 1030–1058.
- (6) Zuo, X.; Subramaniam, B.; Busch, D. H. *Ind. Eng. Chem. Res.* **2008**, 47 (3), 546–552.
- (7) Tomás, R. A. F.; Bordado, J. C. M.; Gomes, J. F. P. *Chem. Rev.* **2013**, 113 (10), 7421–7469.
- (8) Davis, S. E.; Houk, L. R.; Tamargo, E. C.; Datye, A. K.; Davis, R. J. *Catal. Today* **2011**, 160 (1), 55–60.
- (9) Partenheimer, W.; Grushin, V. V. *Adv- Synth. Catal.* **2001**, 343 (1), 102–111.
- (10) Taguchi, Y.; Oishi, A.; Iida, H. *Chem. Lett.* **2008**, 37 (1), 50–51.
- (11) Revankar, V. V. S.; Doraiswamy, L. K. *Ind. Eng. Chem. Res.* **1987**, 26 (8), 1691–1695.
- (12) Revankar, V. V. S. and Doraiswamy, L. K. *Ind. Eng. Chem. Res.* **1987**, 26, 1691–1695.
- (13) Revankar, V. V. S. and Doraiswamy, L. K. *Ind. Eng. Chem. Res.* **1992**, 31, 781–786.
- (14) Ratusky, J.; Tykva, R. and Sorm, F. *Collect. Czechoslov. Chem. Commun.* **1967**, 32 (5), 1719–1729.
- (15) Ratusky, J. *Collect. Czechoslov. Chem. Commun.* **1971**, 36 (8), 2831–2845.
- (16) Raecke, B. *Angew. Chemie* **1958**, 70 (1), 1–36.
- (17) Raecke, B. Ger. Pat. 936,036, 1952.

- (18) J. Sheehan, R. In *Ullmann's Encyclopedia of Industrial Chemistry*; Wiley-VCH Verlag GmbH & Co. KGaA, 2000.
- (19) McNelis, E. *J. Org. Chem* **1965**, *30* (4), 1209–1213.
- (20) van Haveren, J.; Thiyagarajan, S.; Morita, A. T. United States Patent. 9,284,290 B2, 2016.
- (21) Pan, T.; Deng, J.; Xu, Q.; Zuo, Y.; Guo, Q. X.; Fu, Y. *ChemSusChem* **2013**, *6* (1), 47–50.
- (22) Thiyagarajan, S.; Pukin, A.; van Haveren, J.; Lutz, M.; van Es, D. S. *RSC Adv.* **2013**, *3* (36), 15678–15686.
- (23) Troshin, K.; Hartwig, J. F. *Science* **2017**, *357* (6347), 175–181.
- (24) Shevlin, M. *ACS Med. Chem. Lett.* **2017**, *8* (6), 601–607.
- (25) Milo, A.; Neel, A. J.; Toste, F. D.; Sigman, M. S. *Science* **2015**, *347* (6223), 737–743.
- (26) Harper, K. C.; Bess, E. N.; Sigman, M. S. *Nat. Chem.* **2012**, *4* (5), 366–374.
- (27) Fedorov, A.; Liu, H. J.; Lo, H. K.; Copéret, C. *J. Am. Chem. Soc.* **2016**, *138* (50), 16502–16507.
- (28) Engl, P. S.; Santiago, C. B.; Gordon, C. P.; Liao, W. C.; Fedorov, A.; Copéret, C.; Sigman, M. S.; Togni, A. *J. Am. Chem. Soc.* **2017**, *139* (37), 13117–13125.
- (29) Bess, E. N.; Bischoff, A. J.; Sigman, M. S. *Proc. Natl. Acad. Sci.* **2014**, *111* (41), 14698–14703.

- (30) Newhouse, T.; Baran, P. S. *Angew. Chem. Int. Ed.* **2011**, *50* (15), 3362–3374.
- (31) Schuchardt, U.; Cardoso, D.; Sercheli, R.; Pereira, R.; Da Cruz, R. S.; Guerreiro, M. C.; Mandelli, D.; Spinacé, E. V.; Pires, E. L. *Appl. Catal. A Gen.* **2001**, *211* (1), 1–17.
- (32) Sturgeon, M. R.; O'Brien, M. H.; Ciesielski, P. N.; Katahira, R.; Kruger, J. S.; Chmely, S. C.; Hamlin, J.; Lawrence, K.; Hunsinger, G. B.; Foust, T. D.; Baldwin, R. M.; Bidy, M. J.; Beckham, G. T. *Green Chem.* **2014**, *16* (2), 824–835.
- (33) Pineda, A.; Lee, A. F. *Appl. Petrochemical Res.* **2016**, *6* (3), 243–256.
- (34) Luo, H.; Abu-Omar, M. M. *Green Chem.* **2018**.
- (35) Gilkey, M. J.; Xu, B. *ACS Catal.* **2016**, *6* (3), 1420–1436.
- (36) Potyrailo, R.; Maier, W.; Czarnik, A.; Yan, B.; Webster, D.; Schunk, S.; Svedberg, E.; Gao, C.; Woo, D.; Alexanian, A.; Al., E. *Combinatorial and High-Throughput Discovery and Optimization of Catalysts*; Shinar, J., Ed.; CRC Press: Boca Raton, 2006.
- (37) Clark, D. A.; Basile, B. S.; Karnofel, W. S.; Diver, S. T. *Org. Lett.* **2008**, *10* (21), 4927–4929.
- (38) Marshall, J. E.; Keister, J. B.; Diver, S. T. *Organometallics* **2011**, *30* (6), 1319–1321.
- (39) Griffiths, J. R.; Keister, J. B.; Diver, S. T. *J. Am. Chem. Soc.* **2016**, *138* (16), 5380–5391.
- (40) Ricci, A. *Modern Amination Methods*; Wiley: New York, 2007.

- (41) Andersson, P. G.; Schink, H. E.; Österlund, K. *J. Org. Chem.* **1998**, *63* (22), 8067–8070.
- (42) Gill, C. D.; Greenhalgh, D. A.; Simpkins, N. S. *Tetrahedron* **2003**, *59* (46), 9213–9230.
- (43) Magano, J.; Dunetz, J. R. *Org. Process Res. Dev.* **2012**, *16* (6), 1156–1184.
- (44) Kuwano, R.; Takahashi, M.; Ito, Y. *Tetrahedron Lett.* **1998**, *39* (9), 1017–1020.
- (45) Park, S.; Brookhart, M. *J. Am. Chem. Soc.* **2012**, *134* (1), 640–653.
- (46) Cheng, C.; Brookhart, M. *J. Am. Chem. Soc.* **2012**, *134* (28), 11304–11307.

CHAPTER 2. SYNTHESIZING AROMATIC DICARBOXYLIC ACIDS VIA CATALYTIC DISPROPORTIONATION WITH COPPER(I) IODIDE

Modified from a paper to be submitted to a journal

Zachary B. Weinstein, Aaron D. Sadow*

Abstract

Copper(I) iodide catalyzes the disproportionation of aromatic and heteroaromatic carboxylic acids to give dicarboxylic acids. Potassium furoate heated to 280 – 300 °C in the presence of 10 mol% CuI under carbon dioxide (40 bar) forms 2,5-furandicarboxylate in up to 75% yield with excellent selectivity over 2,4-furandicarboxylate (92% selectivity). Potassium benzoate heated to 320 – 350 °C the presence of 10 mol% CuI under carbon dioxide (40 bar) produces terephthalic acid in up to 60% yield.

Introduction

Sustainable manufacturing of aromatic dicarboxylic acids, such as terephthalic acid (TPA) or 2,5-furandicarboxylic acid (2,5-FDCA) used in polyesters, would benefit from non-oxidative syntheses because their bio-renewable precursors are already partially oxidized. These dicarboxylic acid products are intermediates in large scale, or potentially large scale, polymer synthesis. Terephthalic acid (30 million tons per year as of 2006) is primarily used to manufacture poly(ethylene) terephthalate (PET) for applications in textiles and food and beverage containers. Poly(ethylene) furoate (PEF) is an emerging alternative material to PET, with 2,5-FDCA instead of TPA as the dicarboxylate

monomer, because the polyester has the benefit of being less oxygen permeable than PET. Dicarboxylic acids are currently synthesized via harsh oxidation processes from reduced petrochemicals. For example, the multistep Amoco process utilizes *p*-xylene as a precursor to terephthalic acid.^{1,2} A related oxidation of bio-renewable 5-hydroxymethyl furfural (HMF) is proposed for the synthesis of 2,5-FDCA and further enhances the appeal of PEF in the context of sustainability,³ but the short shelf life of HMF may generate challenges for this conversion approach.

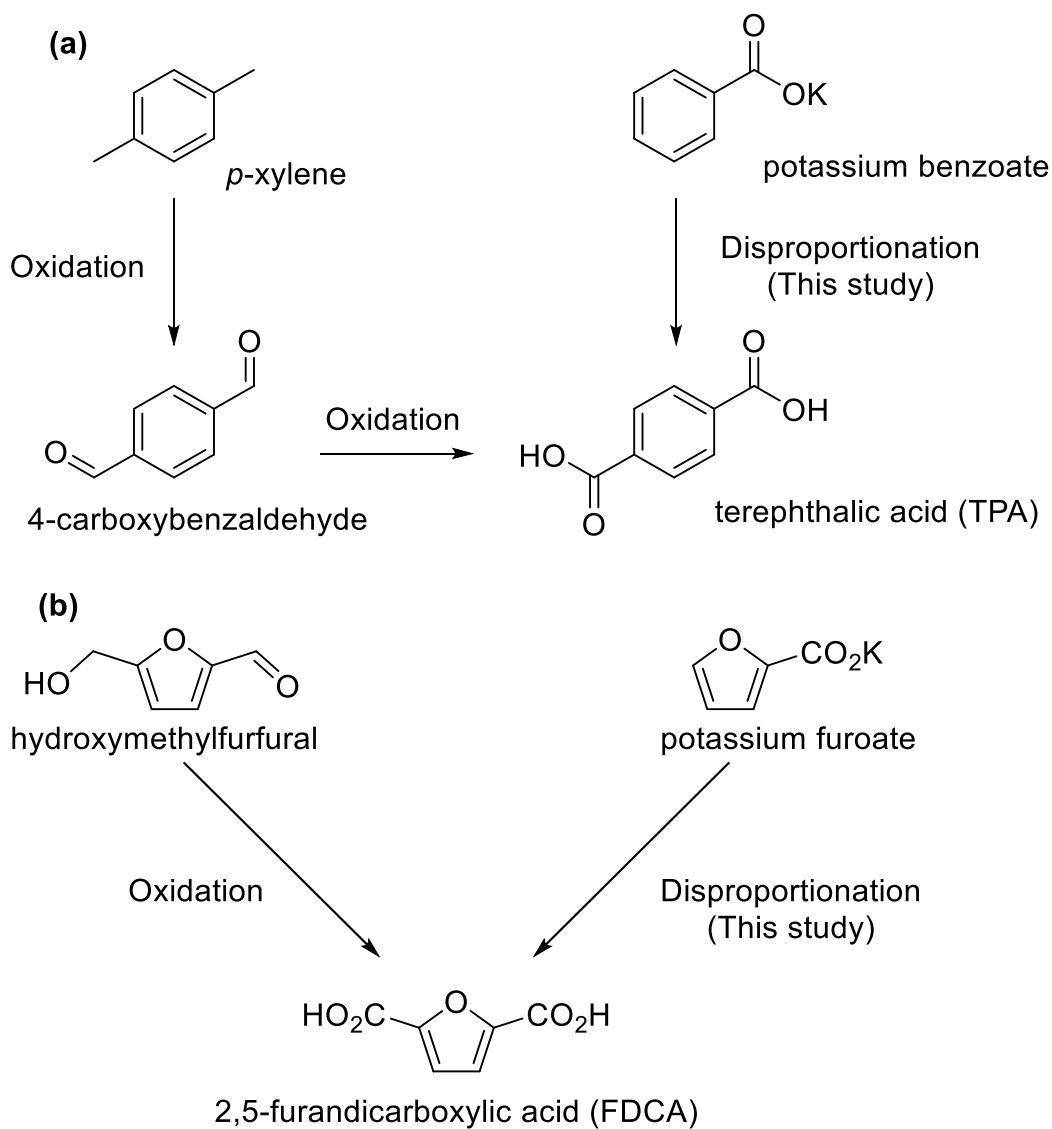
Disproportionation of aromatic monocarboxylates or isomerization of aromatic dicarboxylates could provide an alternative route for the synthesis of isomeric dicarboxylic acids. In fact, the isomerization of isophthalate to terephthalate, known as the Henkel process, was a commercial process prior to the development of the oxidative Amoco process.⁴ The challenges facing the Henkel process include high reaction temperatures, highly toxic cadmium-based catalysts, and variable dependence on carbon dioxide pressure.⁵⁻⁷

The state-of-the-art conditions for disproportionation of potassium benzoate (as described in patent literature)⁸ involve heating solid mixtures of cadmium(II) iodide and potassium benzoate at 350-450 °C under 10-50 bar of CO₂. The isomerization of potassium isophthalate also involves heating mixtures of cadmium(II) iodide and dipotassium isophthalate. Generally, the isomerization reaction occurs at milder temperatures and requires shorter times than disproportionation reaction.⁹ The importance of carbon dioxide in both the disproportionation and isomerization reactions that produce terephthalate appears to be sensitive to the other reaction conditions, and reported carbon dioxide pressures vary widely. Initial reports indicate that the higher pressures of CO₂ are

necessary for conversion,^{10,11} but later studies use atmospheric pressures¹² or even flowing N₂.¹³

Harsh oxidation reactions similar to the Amoco process are used to synthesize 2,5-FDCA from HMF^{14,15,16} and suffer from the same drawbacks as *p*-xylene oxidation. As an alternative to oxidations, Henkel-type disproportionation reactions of furan 2-carboxylate salts may provide 2,5-FDCA. Cadmium iodide catalyzes the redistribution at elevated temperatures (380 °C) under a carbon dioxide atmosphere, similarly to the disproportionation of potassium benzoate. The formation of both 2,5-FDCA and its isomer, 2,4-FDCA (40-59% yield) after 20 min complicate these conversions.^{7,9} Lower temperature (260 °C) and longer reaction time (5.5 h) affords 2,5-FDCA in improved yield (62%) and selectivity (70%) over 2,4-FDCA. In this case, the reaction was performed under flowing N₂.¹³

2,5-FDCA is generally reported to be synthesized at lower temperatures than TPA. A careful study of the effect of temperature on potassium furoate conversion, total FDCA yield, and selectivity for 2,5-FDCA in a ZnCl₂-catalyzed process reveals expectedly that at high conversion with high reaction temperature, product yield decreases from diminished selectivity. Specifically, the yield of 2,5-FDCA increases from 8% in reactions at 220 °C to 52% at 250 °C, but at even higher temperatures and



Scheme 2. Dicarboxylates are often prepared through oxidation. Disproportionation reactions provide an alternative route towards synthesizing diacids. (a) Synthesis of terephthalic acid (b) Synthesis of 2,5-furandicarboxylic acid

higher conversions, yield decreases (e.g., 13% at 280 °C) as a result of poor selectivity.¹⁷ Recently, Kanan and coworkers^{18,19} have developed a novel non-catalytic approach to synthesizing 2,5-FDCA from 2-furoic acid and 1.55 equivalents of Cs₂CO₃ at low temperatures (200 °C) and moderate pressure (8 bar) in good yield (89%). This Cs₂CO₃-mediated pathway provides 2,5-FDCA exclusively, but reactions of benzoic acid and cesium carbonate provide mixtures of diphtalates, triphthalates, and tetraphthalates.

Table 1. Literature evaluation of MX₂ catalyzed furan disproportionation^{13,17}

2		$\xrightarrow[\text{flowing N}_2]{22 \text{ mol } \% \text{ MX}_2}$		+			
	CdCl ₂	<	ZnCl ₂	<	ZnI ₂	<	CdI ₂
Yield (%)	0		31		40		64
Temp (°C)	280		260		260		260
Time (h)	0.5		5.5		5.5		5.5

Several catalysts have been studied in the literature for synthesis of 2,5-FDCA via catalytic disproportionation. When comparing their reported effectiveness toward the disproportionation of potassium furate, the activity trends CdI₂ > ZnI₂ > ZnCl₂ > CdCl₂.^{13, 17} Analysis of the literature indicate that iodide salts of Cd and Zn are more effective catalysts for benzoate disproportionation and isophthalate isomerization than other halides.^{7,20,21} Thus, the d¹⁰ metal center and iodide counterion were identified as

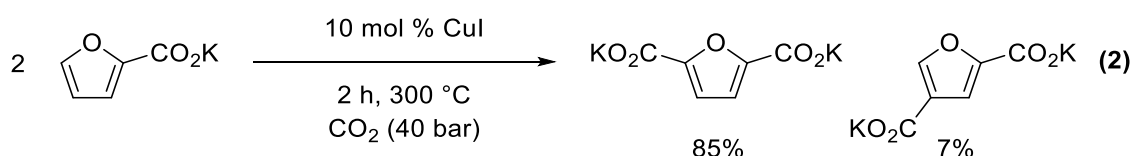
important components, and we were curious whether CuI would be effective in the Henkel reaction as transition-metal based, monovalent alternative to the group 12 catalysts. Notably, the d^9 salt CuCl_2 is not effective for the synthesis of 2,5-FDCA under the same conditions as CdI_2 .¹³

In order to access dicarboxylic acids from bio renewable sources and provide a better route to 2,5-FDCA towards sustainable PEF, we sought to discover cadmium-free, highly selective catalytic conditions for disproportionation or isomerization of aromatic carboxylates. We have studied CuI mediated disproportionation of potassium furoate to 2,5-FDCA to advance this approach. The principles we have found from furoate disproportionation are applicable to other aromatic carboxylates, as well as isomerization of dicarboxylates.

Results and Discussion

The Henkel reaction occurs at high temperatures at a solid-solid interface of an inhomogeneous mixture of substrate and catalyst. To mitigate heat transfer issues and temperature gradients that might influence reproducibility, we fabricated an aluminum insert for a stainless-steel Parr autoclave reactor with evenly distributed slots for four glass reaction vessels and a position for a thermocouple. This reactor configuration allows parallel reactions, with the temperature of the aluminum insert governing the temperature in each reactor vessel. Reactions performed in parallel under the conditions of equation 1 established good reproducibility within three reactors in a single experiment (yield = $75 \pm 2\%$), and multiple experiments demonstrate good reproducibility between

The insoluble material contained species derived from the copper catalyst and pyrolyzed organics, which account for a portion of the lower-than-theoretical yield. ^1H NMR spectra in $\text{DMSO-}d_6$ of the soluble portion contained broad signals and could not be used to accurately quantify the products present. Instead, acidification of the aqueous solution precipitated pure 2,5-FDCA (75% isolated yield). Analysis of the remaining soluble portion by ^1H NMR spectroscopy revealed 2,4-FDCA (7% yield), 2,5-FDCA (10% yield) and trace furoic acid (<1%).



The product yields are sensitive to the reaction temperature. The isolated yield of 2,5-FDCA increases from 0 to 75% as the reaction temperature increases from 260 – 300 °C (**Table 2**). The maximum isolated yield of 2,5-FDCA is obtained in reactions heated at 300 °C. More insoluble black materials form and isolated yields of 2,5-FDCA decrease at temperatures above 300 °C.

Carbon dioxide appears to have a number of roles in the reaction. First, it is needed for conversion to occur. Reaction mixtures after thermal treatment of potassium furoate under high pressure of N_2 (60 bar) but in the absence of CO_2 contain only starting materials, even in the presence of the CuI catalyst. As noted above, potassium furoate is also recovered quantitatively in experiments that lack copper iodide. Thus, we conclude

Table 2. Temperature effects on CuI-catalyzed furoate disproportionation, assessed by % yield of isolated 2,5-FDCA.

Temp (°C) ^a	Isolated Yield of 2,5-FDCA (%) ^b
260	0
280	20 (± 2)
290	70 (± 2)
300	75 (± 1)
310	67 (± 1)

^a1.75 mmol potassium furoate, 0.18 mmol CuI, 2 h under CO₂ (40 bar). ^bAverage of 3 reactions

that CO₂ and CuI interact to generate an active catalytic species. In addition, conversion increases as carbon dioxide pressure increases. For example, approximately 50% of potassium furoate is converted in experiments under only 1 bar of CO₂, whereas 73% conversion is observed with 10 bar of CO₂ under otherwise equivalent conditions. Second, the CO₂ pressure affects the yield by favoring the dicarboxylate product. 2,5-FDCA yields are lower in experiments with lower CO₂ pressure and higher with increased pressure (**Table 3**). For example, the only isolable species after thermolysis under 1 bar of CO₂ is the starting material, and 2,5-FDCA is not formed in detectable quantities even though half of the potassium furoate reacts. Increased pressure of CO₂ to

10 bar increases the 2,5-FDCA yield to 33%. More intractable black materials are formed in these low CO₂ pressure experiments than those at 40 bar of CO₂, suggesting that the amount of carbon dioxide affects the accessible reaction pathways. Moreover, higher carbon dioxide pressure also inhibits decomposition of the 2,5-FDCA product.

Thermolysis of dipotassium 2,5-furandicarboxylate under only 1 bar of CO₂ (in the presence of CuI) results in a 20% loss of starting material after 1 h, whereas the 2,5-FDCA yields at 40 bar are identical after 1 h and 18 h (see Table 4 below).

Decomposition likely occurs from both the carboxylate and the dicarboxylate under low pressure of CO₂. Because both starting material and products contain carboxylate moieties and similar trends are observed in potassium benzoate disproportionation reactions, we infer that the decomposition pathway to intractable black materials involves loss of the carboxylate moiety.

Table 3. Pressure effects on CuI-catalyzed furoate disproportionation, assessed by % yield of isolated 2,5-FDCA.

CO ₂ Pressure (bar) ^a	Total Yield of 2,5-FDCA (%) ^c
1	0 (0) ^d
10	33 (0) ^e
40	85 (75)

Table 3. (continued)

N ₂ pressure (bar)	
60 ^b	0 (0)

^a1.75 mmol potassium furoate, 0.18 mmol CuI, 300 °C, 1 h. ^bNitrogen used in place of CO₂. ^cparenthesis indicate isolated yield ^d47% starting material ^e27% starting material

The time dependencies of conversion and yield are not equivalent, suggesting that the formation of 2,5-FDCA proceeds through a multistep pathway involving a less reactive intermediate than the starting materials. First, conversion of potassium furoate occurs rapidly at 300 °C. After 5 minutes, 95% of starting material is consumed and within 30 minutes conversion is essentially complete (>99%, **Table 4**). Although conversion is high after 5 minutes, total 2,5-FDCA yield is only 65% of the theoretical yield. Longer reaction times give increased yield, to 81% after 30 minutes and 85% after 1 hour, at which point the reaction is complete. The yield remains constant even as the reaction mixture is held at 300 °C for 18 hours. This consistency over time indicates that the decomposition pathway is not accessible by dicarboxylates at 300 °C under 40 bar CO₂. As noted above, yields decrease at temperatures above 300 °C as a decomposition pathway is accessed, and more intractable black material is formed.

As noted above, 2,4-FDCA is produced as a side product in this reaction. Selectivity is calculated based on 2,5-FDCA yield vs 2,4-FDCA yield. The selectivity is significantly higher (92%) than the previous state-of-the-art CdI₂ based catalyst (70%).¹³ Although yields drop at higher temperatures, selectivity remains constant. As catalyst

loading is increased, isolated yield of 2,5-FDCA decreases, as selectivity for 2,5- vs 2,4-FDCA decreases as well. At 25 mol % catalyst, isolated yield of 2,5-FDCA drops to 66% as selectivity drops to 71%. As the catalyst loading increases to 100% (stoichiometric catalyst), a very large amount of intractable black material forms, and no 2,5-FDCA is isolated. In these experiments, the selectivity of the crude mixture decreases to 41% (by ^1H NMR in D_2O). In experiments when the catalyst loading is decreased below 10%, marginal increases to selectivity may be observed, but the reaction does not go to full conversion.

Table 4. Reactions of potassium furoate with 10 mol % CuI at 300 °C under CO_2 (40 bar) varying conditions for time and temperature.

Time (at 300 °C) ^a	Conversion (%) ^b	Diacid Yield (%) ^c	Total yield of 2,5-FDCA (%) ^d	Selectivity for 2,5- vs 2,4-FDCA (%) ^e	Isolated Yield (%) ^f
5 min	95 (± 2)	74 (± 4)	65 (± 3)	87	44 (± 1)
30 min	>99	87 (± 4)	81 (± 3)	93	71 (± 2)
1 h	>99	92	85	92	76 (± 2)

Table 4. (continued)

18 h	>99	92	85	92	75 (\pm 1)
1 h ^f	>99	85	78	92	61 (\pm 1)

^aThis refers to the elapsed time at the designated temperature. The reactor requires roughly 50 minutes to heat to the designated temperature. ^bTotal % conversion of potassium furoate ^c% Yield of total 2,4-FDCA and 2,5-FDCA combined from isolate and supernatant ^d% Yield of total 2,5-FDCA from isolate and supernatant ^e[% yield of 2,5-FDCA/% yield of combined FDCA] X 100 ^f% Yield of pure washed 2,5-FDCA ^gReactor temperature at 320 °C

Although most reported Henkel-type reactions use potassium carboxylates for disproportionation, sodium furoate was identified as a possible starting material for the synthesis of 2,5-FDCA in experiments using ZnCl₂ as a catalyst (2,5-FDCA forms in 15% yield after 3 h at 250 °C)¹⁷ In this CuI-catalyzed system, sodium furoate is effective as a metal carboxylate precursor as well, with competitive yields of 2,5-FDCA compared reactions of potassium furoate with CdI₂ catalysts. As discussed above, reactions of potassium furoate with CuI require temperatures of 280-300 °C. Sodium furoate disproportionation catalyzed by CuI requires temperatures above 300 °C. Sodium furoate heated to 300 °C for 2 h returns only starting material. At 320 °C, 2,5-FDCA increases to 10% and at 340 °C, yield further increases to 59% (**Table 5**).

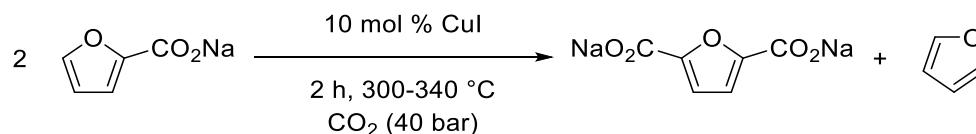


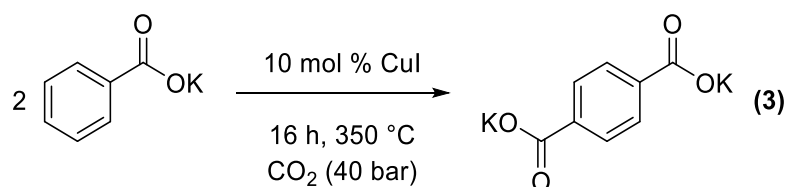
Table 5. Temperature effects on CuI-catalyzed sodium furoate disproportionation, assessed by % yield of isolated 2,5-FDCA.

Temperature (°C)	Isolated Yield of 2,5-FDCA (%)
300	0
320	10
340	59

Conditions: 10 mol % CuI, CO₂ (40 bar), 2 h

Copper(I) iodide is also an effective catalyst for the disproportionation of potassium benzoate. As noted above, benzoate disproportionation reactions typically occur at higher temperatures than furoate disproportionation. Heating potassium benzoate to 350 °C under 40 bar of CO₂ in the presence of 10 mol % CuI reacts to form terephthalic acid in 60% yield after 16 hours (Eq. 3). Temperatures above 350 °C could not be tested due to limitations with the autoclave reactor. Similar experiments were

attempted with sodium benzoate, but at 350 °C starting material is recovered quantitatively.



Copper(I) iodide was also investigated as a potential catalyst for the isomerization of dipotassium isophthalate in the synthesis of terephthalate (**Table 6**). Under similar conditions used for potassium benzoate disproportionation (Eq. 3), terephthalic acid is recovered from isophthalate isomerization in 21.4% yield. Interestingly, terephthalic acid yield is only 21.4% while conversion of starting material is 46.6%. The unaccounted-for material can be attributed to black intractable precipitate. Isophthalic acid and terephthalic acid have similar solubility making the workup more challenging, as the acidified product is a mixture of both isophthalic and terephthalic acid. The product to starting material ratio of the acidified mixture was determined by spectroscopy. Disodium isophthalate was also investigated as a starting material, but no conversion occurred at 350 °C. Sodium benzoate and disodium isophthalate have been reported to be converted to terephthalate in the presence of CdI_2 , although they require temperatures of 450 °C.²²

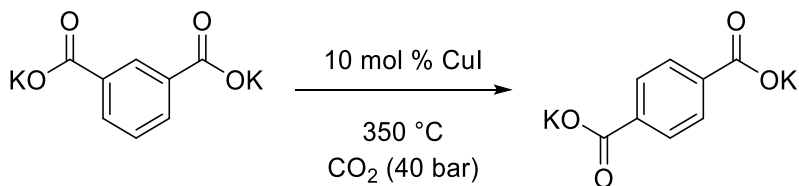


Table 6. Reaction of dipotassium isophthalate to terephthalate as various times.

Time (h)	Conversion (%) ^a	Isophthalic Acid (%) ^b	Terephthalic Acid (%) ^c
1	15.5	84.5	0
3	45.8	54.2	14.5
16	46.6	53.4	21.4

Conditions: 10 mol % CuI, CO₂ (40 bar), 350 °C, run in triplicate. ^a% conversion of isophthalate ^b% recovery of isophthalic acid ^c% yield of terephthalic acid

Conclusion

In conclusion, we have developed methods for utilizing CuI, an inexpensive, commercially available catalyst for disproportionation and isomerization of aromatic carboxylates to dicarboxylates. Compared to the previous state-of-the-art with CdI₂, total yield of 2,5-FDCA has increased to 85% in 1 h versus from 64% in 5.5 h with CdI₂. The drawbacks for CuI is the increased reaction temperature to 300 °C from 260 °C and the need for high pressures of CO₂. CO₂ appears to be involved in the catalytic pathway, due to the lack of conversion in the absence of CO₂, under N₂ conditions. The high pressures of CO₂ required imply that CO₂ acts to activate the catalyst, as well as stabilize the intermediate and inhibit decomposition. The amount of catalyst plays a significant role in

the selectivity of 2,5- vs 2,4-FDCA, as increased catalyst concentration favors 2,4-FDCA, but in instances when the catalyst concentration is too low, the reaction doesn't reach full conversion as the catalyst is not mobile during the reaction. Potassium benzoate and dipotassium isophthalate are also able to be converted to terephthalate under analogous conditions. Finally, we have discovered that CuI can catalyze the disproportionation of sodium furoate as well, albeit at higher temperatures than the potassium analog. These reactions can potentially provide a new non-oxidative pathway for the synthesis of 2,5-FDCA which has commercial applications for polymer synthesis.

Experimental

Synthesis of 2,5-furan dicarboxylic acid from potassium furoate

Dried potassium furoate (262 mg, 1.75 mmol) was ground together with copper (I) iodide (33 mg, 0.17 mmol) into a clean test tube. The test tube was placed in an aluminum block inside of a Parr reactor. The reactor was charged and vented with CO₂ three times to remove air. After degassing for the final time, the reactor was charged with CO₂ (40 bar). The reactor was placed in a heating mantle and heated to 300 °C for 16 hours and then cooled to room temperature.

The reactor was vented slowly and the reddish-black solid was removed from the test tube, and dissolved in hot water. The solution was filtered through a small charcoal layer over a glass filter plug, and was acidified with HCl (aq) precipitating out a white solid. After standing for one hour, the mixture was centrifuged, the supernatant decanted, and the solid washed with water.

The white solid was dried, yielding pure 2,5 FDCA (73.5 mg, 0.47 mmol). The supernatant and wash solutions were combined. After extraction with DMSO, it was determined that the wash solutions contained KCl (118.3 mg, 1.59 mmol), furoic acid (5.6 mg, 0.05 mmol), 2,4 FDCA (8.3 mg, 0.05 mmol) and 2,5 FDCA (31.0 mg, 0.20 mmol). The materials in total yielded 78.5 % 2,5 FDCA with 85 % recovery of organic furoates, and 90.8 % yield of KCl.

Synthesis of 2,5-furan dicarboxylic acid from sodium furoate

Dried sodium furoate (235 mg, 1.75 mmol) was ground together with copper (I) iodide (33 mg, 0.17 mmol) into a clean test tube. The test tube was placed in an aluminum block inside of a Parr reactor. The reactor was charged and vented with CO₂ three times to remove air. After degassing for the final time, the reactor was charged with CO₂ (40 bar). The reactor was placed in a heating mantle and heated to 340 °C for 2 hours and then cooled to room temperature.

The reactor was vented slowly and the reddish-black solid was removed from the test tube, and dissolved in hot water. The solution was filtered through a small charcoal layer over a glass filter plug, and was acidified with HCl (aq) precipitating out a white solid. After standing for one hour, the mixture was centrifuged, the supernatant decanted, and the solid washed with water.

The white solid was dried, yielding pure 2,5 FDCA (80 mg, 0.51 mmol, 58.3 % yield).

Synthesis of terephthalic acid from potassium benzoate

Dried potassium benzoate (108 mg, 0.67 mmol) was ground together with copper (I) iodide (13 mg, 0.07 mmol) into a clean test tube. The test tube was placed in an

aluminum block inside of a Parr reactor. The reactor was charged and vented with CO₂ three times to remove air. After degassing for the final time, the reactor was charged with CO₂ (40 bar). The reactor was placed in a heating mantle and heated to 350 °C for 2 hours and then cooled to room temperature.

The reactor was vented slowly and the reddish-black solid was removed from the test tube, and dissolved in hot water. The solution was filtered through a small charcoal layer over a glass filter plug, and was acidified with HCl (aq) precipitating out a white solid. After standing for one hour, the mixture was centrifuged, the supernatant decanted, and the solid washed with water.

The white solid was dried, yielding terephthalic acid (28 mg, 0.17 mmol, 50.7 % yield).

Synthesis of terephthalic acid from dipotassium isophthalate

Dried dipotassium isophthalate (188 mg, 0.78 mmol) was ground together with copper (I) iodide (15 mg, 0.08 mmol) into a clean test tube. The test tube was placed in an aluminum block inside of a Parr reactor. The reactor was charged and vented with CO₂ three times to remove air. After degassing for the final time, the reactor was charged with CO₂ (40 bar). The reactor was placed in a heating mantle and heated to 350 °C for 3 hours and then cooled to room temperature.

The reactor was vented slowly and the reddish-black solid was removed from the test tube, and dissolved in hot water. The solution was filtered through a small charcoal layer over a glass filter plug, and was acidified with HCl (aq) precipitating out a white solid.

After standing for one hour, the mixture was centrifuged, the supernatant decanted, and the solid washed with water.

The white solid was dried, yielding a mixture of terephthalic acid and isophthalic acid at a ratio of roughly 1:4 respectively by ^1H NMR spectroscopy (90 mg, 0.54 mmol, 69 % recovery).

References.

- (1) J. Sheehan, R. In *Ullmann's Encyclopedia of Industrial Chemistry*; Wiley-VCH Verlag GmbH & Co. KGaA, 2000.
- (2) Zuo, X.; Subramaniam, B.; Busch, D. H. *Ind. Eng. Chem. Res.* **2008**, *47* (3), 546–552.
- (3) Bozell, J. J.; Petersen, G. R. *Green Chem.* **2010**, *12* (4), 539.
- (4) Weissermel, K.; Arpe, H.-J. In *Industrial Organic Chemistry*; Wiley-VCH Verlag GmbH, 2003; pp 388–405.
- (5) Ratusky, J. *Collect. Czechoslov. Chem. Commun.* **1972**, *37* (7), 2436–2450.
- (6) Ratusky, J. *Chem. Ind.* **1970**, No. 42, 1347–1349.
- (7) Ratusky, J.; Tykva, R. and Sorm, F. *Collect. Czechoslov. Chem. Commun.* **1967**, *32* (5), 1719–1729.
- (8) Raecke, B. Ger. Pat. 936,036, 1952.
- (9) Ratusky, J. *Collect. Czechoslov. Chem. Commun.* **1971**, *36* (8), 2831–2845.

- (10) Raecke, B. *Angew. Chemie* **1958**, *70* (1), 1–36.
- (11) Wang, Z. *Comprehensive Organic Name Reactions and Reagents*, 3rd ed.; John Wiley & Sons, Inc.: Hoboken, NJ, 2009.
- (12) Ogata, Y.; Tsuchida, M.; Muramoto, A. *J. Am. Chem. Soc.* **1957**, *79* (22), 6005–6008.
- (13) Thiyagarajan, S.; Pukin, A.; van Haveren, J.; Lutz, M.; van Es, D. S. *RSC Adv.* **2013**, *3* (36), 15678–15686.
- (14) Partenheimer, W.; Grushin, V. V. *Adv- Synth. Catal.* **2001**, *343* (1), 102–111.
- (15) Davis, S. E.; Houk, L. R.; Tamargo, E. C.; Datye, A. K.; Davis, R. J. *Catal. Today* **2011**, *160* (1), 55–60.
- (16) van Haveren, J.; Thiyagarajan, S.; Morita, A. T. United States Patent. 9,284,290 B2, 2016.
- (17) Pan, T.; Deng, J.; Xu, Q.; Zuo, Y.; Guo, Q. X.; Fu, Y. *ChemSusChem* **2013**, *6* (1), 47–50.
- (18) Banerjee, A.; Dick, G. R.; Yoshino, T.; Kanan, M. W. *Nature* **2016**, *531* (7593), 215–219.
- (19) Dick, G. R.; Frankhouser, A. D.; Banerjee, A.; Kanan, M. W. *Green Chem.* **2017**, *19* (13), 2966–2972.
- (20) Revankar, V. V. S. and Doraiswamy, L. K. *Ind. Eng. Chem. Res.* **1987**, *26*, 1691–1695.

- (21) Revankar, V. V. S. and Doraiswamy, L. K. *Ind. Eng. Chem. Res.* **1992**, 31, 781–786.
- (22) Ratusky, J. *Collect. Czechoslov. Chem. Commun.* **1973**, 38 (1), 74–86.

CHAPTER 3. UNIQUE APPROACHES TO CATALYSIS ON AN AUTOMATED SYNTHESIS PLATFORM

Modified from a paper to be submitted to a journal

Zachary B. Weinstein, Dr. Regina R. Reinig, Bradley M. Schmidt, Dr. Hui Zhou, Pranjali Naik, Dr. Igor I. Slowing, Dr. Aaron D. Sadow*

Abstract

Herein we describe the use of an automated synthesis platform (Chemspeed SWING-XL) to develop methods for studying chemical kinetics, synthesis of heterogeneous catalysts and the preparation of synthetically challenging butadiene derivatives. Kinetics of [tris(oxazolinyl)borato]cobalt catalyzed cyclohexane oxidation was studied in detail through automated sampling and quenching of a small library of reactions.

Heterogeneous catalysts were prepared through iterative additions of a Pd solutions onto SiO₂, TiO₂, CeO₂ and Al₂O₃ supports which were used in hydrogenation reactions.

Specialized high-pressure pumps were used to dispense fresh catalyst solutions into a heated, pressurized reactor to optimize the yield of functionalized butadiene monomers.

Other Author's Contributions

Regina Reinig: Responsible for synthesis of To^MMX catalysts and reaction analysis.

Bradley Schmidt: Responsible for preparation and analysis of enyne metathesis experiments.

Hui Zhao: Responsible for synthesis of CeO₂ and experimentation and analysis of hydrogenolysis reactions of guaiacol.

Pranjali Naik: Analysis of heterogeneous catalysts by ICP-MS and Chemisorption.

General Introduction

The growth of automation is gaining influence in all facets of life, economy, industry and technology. As new technologies advance, development of new methods is required to utilize these technologies to their fullest capability. Wide-spread prominence of automation is appearing across all fields, including the field of Chemistry, from fabrication of 3D printed reactors¹⁻³ to its emergence in the form of high-throughput experimentation (HTE).⁴⁻¹⁰ To maximize output from these new instruments, we seek to develop new methods to not only increase productivity but allow us to perform novel experiments which would otherwise prove impossible without the instrument. Using this technology, novel reactions can be performed round the clock, limiting human error, increasing data points and running parallel reactions to minimize variance.

High-throughput experimentation is typically used for assessing the effect of a specific reaction parameter on yield and/or selectivity.¹¹⁻¹⁵ While these types of experiments can give optimized conditions for a specific parameter, full reaction optimization can be more difficult to determine. Fortunately, more unique methods of experimentation are being developed to get more useful information from these advanced technologies. Sigman and coworkers have used mathematical correlations between quantifiable properties of a catalyst ligand interaction to predict and optimize

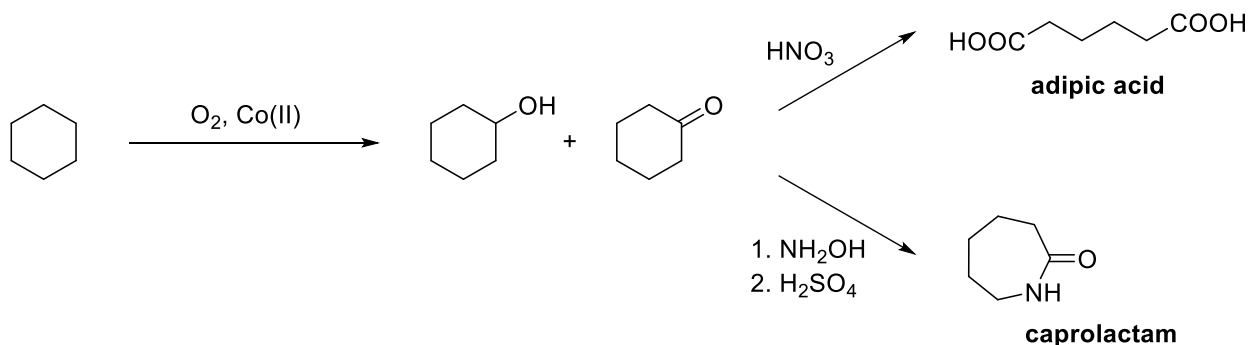
enantioselectivity of a reaction.⁶ Hartwig and coworkers describe a technique titled Snap Deconvolution which allows multiple reactants to be mixed in one vessel, and subsequently analyzed automatically by mass spectrometry.⁹ These Design of Experiment (DOE) type experiments are popular methods of optimizing a reaction. It involves mapping a quantifiable result against secondary interactions as a means to optimize a system. This method identifies a system over the sum of its individual parts. A more accurate and detailed assessment can be made by changing variables individually. Herein we describe our strategies of studying the kinetic profile of a reaction and methods for preparing heterogeneous catalysts.

Introduction: Chemical Kinetics

Determining the chemical kinetic landscape of a reaction is invaluable to discovering mechanistic information. To determine a rate law, a reaction needs to be monitored at a specific set of conditions/parameters. Variables such as concentration, solvent, temperature and substrates can all effect the k , rate constant. Acquiring data points to establish a rate law at a specific set of conditions can be complicated and/or time consuming, if not tedious. Determining the rate under multiple variables, exponentially more experiments need to be performed, increasing the difficulty of accruing all the appropriate data. Establishing a method of performing these experiments and accumulating all the data would be invaluable. Automation provides a way to study a reaction modifying multiple variables simultaneously to determine a broad chemical kinetic profile, at a low cost of man-hours. Using a high-throughput robot, we can acquire the data for multiple kinetic reactions simultaneously, altering some parameters which

keeping others stable. Understanding all these details provide detailed mechanistic insight and allow optimization of a rate of reaction.

Selective or partial oxidation of aliphatic alkanes can be challenging.¹⁶ Cobalt is often used industrially as an oxidation catalyst¹⁷ and has more recently been demonstrated to be efficient at more selective oxidations.¹⁸ These oxidations are incredibly useful industrially, as they can be used to synthesize adipic acid and caprolactam, vitally important commodities in the nylon industry (Scheme 1).¹⁹



Scheme 1. Conversion of Cyclohexane to Adipic Acid or Caprolactam

Regina Reinig began to synthesize a series of [tris(oxazoliny)borato]cobalt compounds, which showed catalytic activity towards oxidation of aliphatic alkanes.²⁰ Preliminary studies of this reaction gave encouraging results, showing favorable selectivity towards the alcohol, as opposed to the overoxidized ketone side-product. We were interested in studying the kinetics of this reaction, to develop a broad understanding of the system and subsequently be able to optimize the reaction. As multistep oxidations can require a lot of data to fully interpret (Figure 1) we worked to develop a method to acquire as much data as possible as we began to study the kinetics of the oxidation of

aliphatic alkanes to alcohols and ketones earth abundant first row transition metal catalysts.

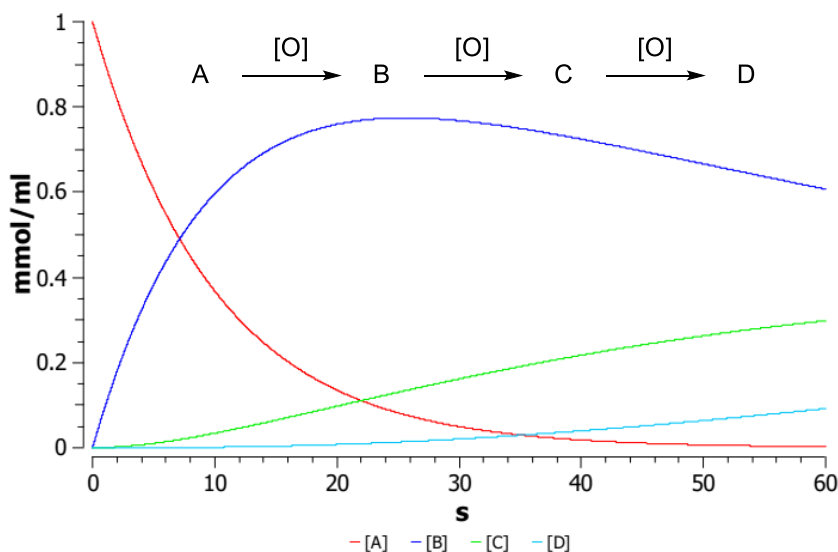


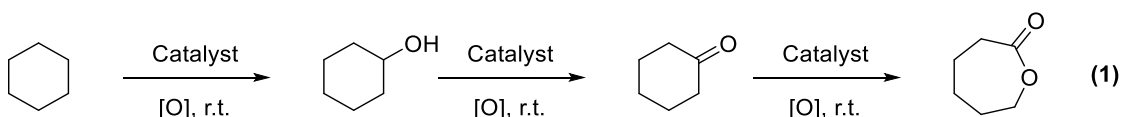
Figure 1. Kinetic Trace of a Generic 3 Step Oxidation Reaction (Simulated using COPASI)

Results and Discussion: Chemical Kinetics

Using our unique Chemspeed SWING-XL synthetic robot, we devised a strategy for automated sampling of parallel reactors to quench reactions at specific time intervals. A small library was assembled varying either catalyst, concentration, solvent or oxidant while running parallel reactions in triplicate to minimize error and assess instrument precision. Our strategy involved time-controlled sampling of a reaction directly into a small sampling vial. As these oxidation reactions occur at room temperature, we needed a

method to immediately quench the samples to prevent the reaction from continuing in the sampling vials.

The majority of these experiments utilized hydrogen peroxide as the oxidant. We required a quenching agent which would quickly decompose or quench hydrogen peroxide, without affecting the overall reaction. Potassium iodide was an intriguing option as a decomposition catalyst, as KI is a well-known catalyst to decompose H_2O_2 to H_2O and O_2 . Unfortunately, this catalytic decomposition caused several issues. First, it was exothermic which led to solvent, substrate and product evaporation. Secondly, we discovered that it also catalyzed side-reactions with the cyclohexylperoxy intermediate. Between these two issues, conversion and yield was difficult to assess. After thoughtful analysis we chose to use stoichiometric triphenylphosphine as a reducing agent, as it rapidly consumes H_2O_2 as it oxidizes into triphenylphosphine oxide. This quenching reaction is also fairly exothermic, but when the PPh_3 was dissolved in solution, we found that the extra solvent helps mitigate heat issues. This method also avoided any unwanted side reactions.



After determining a sampling and quenching technique, we begin to study the kinetics of cyclohexane oxidation (Eq. 1) using a series of cobalt catalysts at three concentrations. We used an 8-mL vial array from the instrument, and tested CoCl_2 , $\text{To}^{\text{M}}\text{CoCl}$ and $\text{To}^{\text{M}}\text{CoOAc}$ as catalysts with catalyst amounts of 1, 3 and 5 μmol (0.16, 0.48 and 0.80 mM) (Figure 2). Zero-time samples were taken immediately after

introduction of the oxidant, and subsequent samples were taken sequentially over time. The time samples were analyzed by GC-FID with an internal standard, and the rate constant of the first and second oxidation was determined for each experiment (Figure 3). The integrity of this method was analyzed by comparing the rate constants over multiple identical experiments (Table 1). While each individual time point may have a small amount of error involved in the handling or the GC calibration, once all the points are plotted versus time the magnitude of the errors are minimized and the standard deviation of the rate constants is very small ($k_1 = 1.19 \times 10^{-6} \text{ M/s}$, $k_2 = 1.41 \times 10^{-4} \text{ M/s}$).

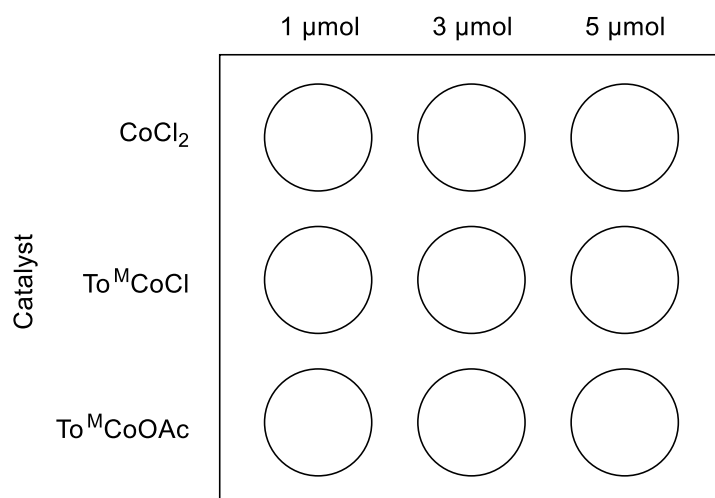


Figure 2. Reactor array of cobalt catalysts with multiple catalyst loadings

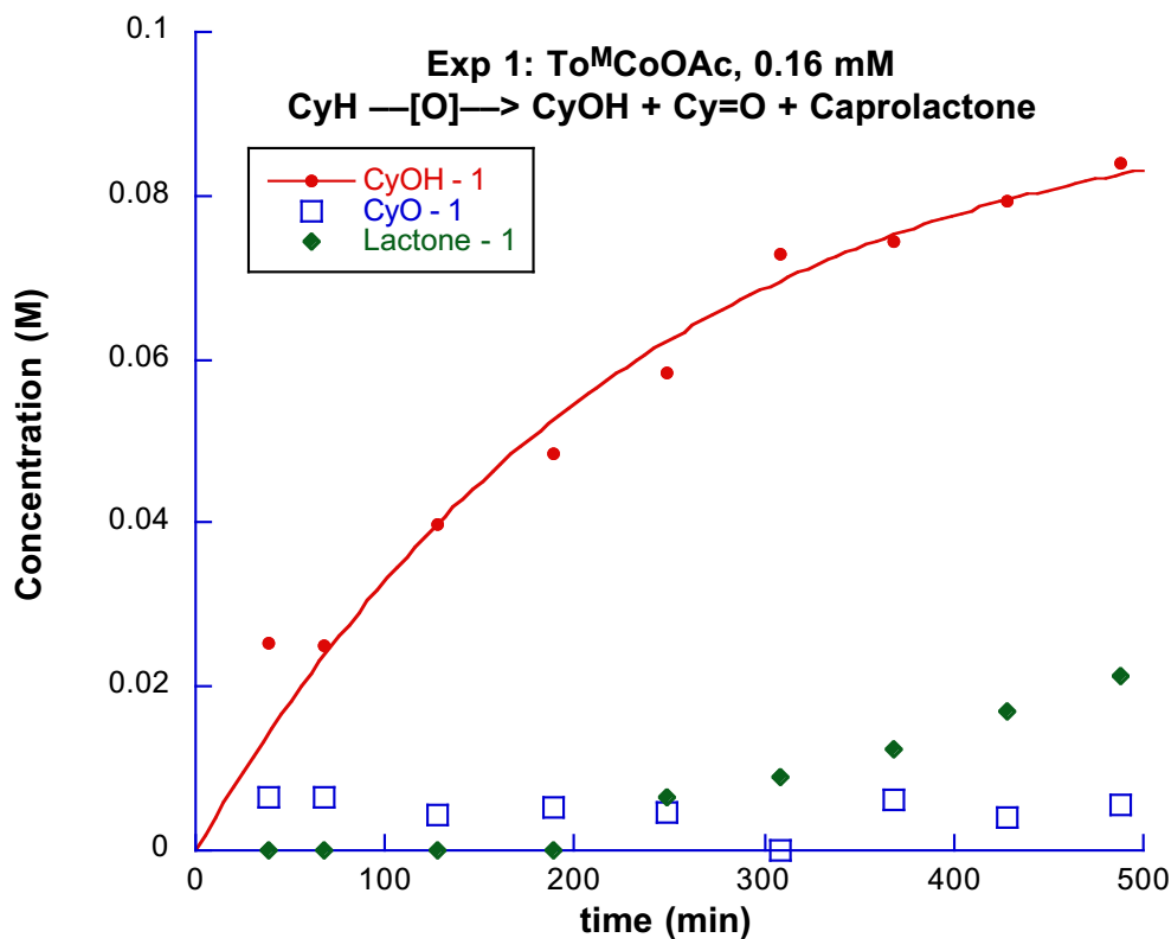


Figure 3. Kinetic Trace of Cyclohexane Oxidation Catalyzed by To^MCoOAc.

Conditions: Cyclohexane (1.6 mL, 15 mmol, 2.45 M) oxidation catalyzed by To^MCoOAc (1 μ mol, 0.16 mM) in dichloromethane/acetonitrile (95%, 1 mL) in the presence of *m*CPBA (345 mg, 2.0 mmol) at 25 °C over 24 hours.

Table 1. Reproducibility of Kinetic Data as Evidenced by Rate Constants

Experiment	k_1 (M/s)	k_2 (M/s)
1	0.0001641	0.003948
2	0.0001645	0.003803
3	0.0001668	0.004147
Average	0.0001651	0.003966
Std. Dev.	1.19×10^{-6}	1.41×10^{-4}

Conditions: Cyclohexane (1.6 mL, 15 mmol, 2.45 M) oxidation catalyzed by $\text{To}^{\text{M}}\text{CoOAc}$ (1 μmol , 0.16 mM) in dichloromethane/acetonitrile (95%, 1 mL) in the presence of *m*CPBA (345 mg, 2.0 mmol) at 25 °C over 24 hours.

After gaining confidence in our method, we analyzed a series CoX_2 salts as catalysts for cyclohexane oxidation (Figure 4). CoCl_2 , $\text{To}^{\text{M}}\text{CoCl}$ and $\text{To}^{\text{M}}\text{CoOAc}$ were the catalysts tested using the same method used to determine the rate constants. All three catalysts have similar % selectivity towards cyclohexanol, reaching the highest selectivity around the 2 h mark (85-90%) which slowly decreases as cyclohexanone and caprolactone are produced. $\text{To}^{\text{M}}\text{CoOAc}$ is the most active catalyst, having the highest turnover numbers (TON) for cyclohexane at 86 turnovers.

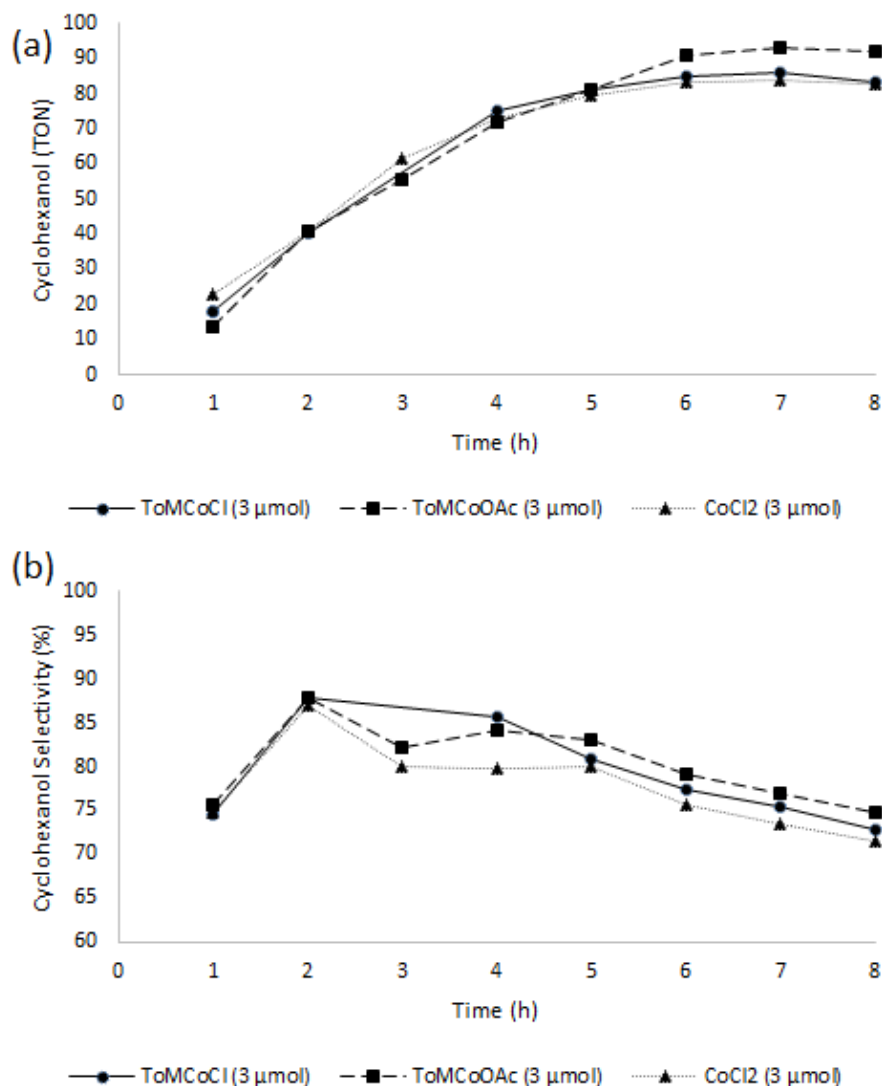


Figure 4. Comparison of Cobalt(II) Catalysts for Cyclohexane Oxidation (a) Effect of Catalyst on Cyclohexanol Turnover Numbers (b) Effect of Catalyst on Cyclohexanol Selectivity (%)

We began to investigate other first row transition metals, studying Fe and Ni compounds in analogous oxidation reactions to the conditions described above. We found

To^MNiOAc to be a more selective catalyst towards cyclohexanol conversion than To^MCoOAc. To^MFeOAc was also tested as a catalyst, but found to be less selective towards cyclohexanol conversion than the Co and Ni analog.

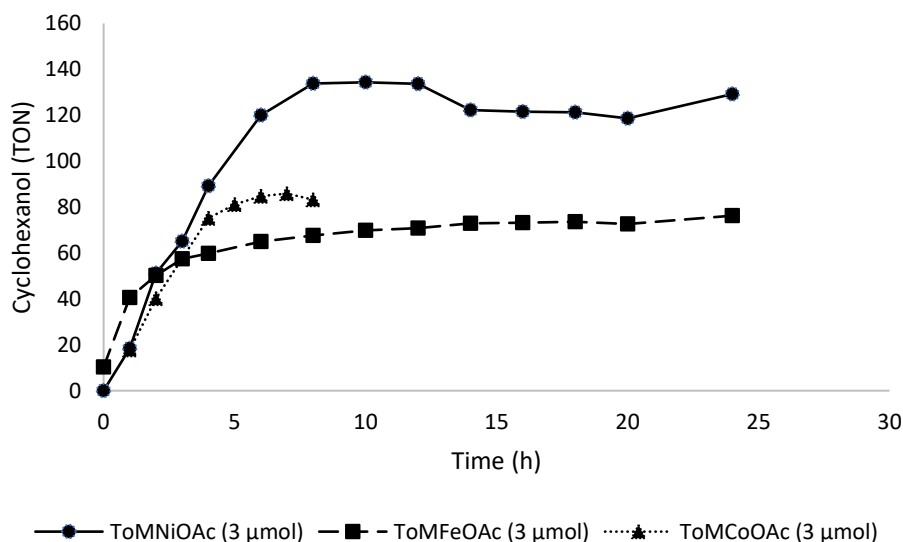


Figure 5. Comparison of Several To^MMOAc Catalysts for Cyclohexanol Conversion

We began to expand the scope of our reactions to other oxidants as well, but had issues with using aqueous oxidants. When H₂O₂ was used as an oxidant in place of *m*CPBA, we were unable to acquire any reproducible data. Multiple samples acquired within a single time-point would have a broad range of yield and selectivity. As everything within the reaction mixture appeared to be a monophasic solution, but our GC analysis was not giving us reliable data, we attempted to study the yield and selectivity via Raman spectroscopy. Jonathan Bobbitt in Dr. Emily Smith's research group studied the reaction under light microscopy and Raman spectroscopy (Figure 6). We quickly learned that although the solution appeared uniform and monophasic, small micelles were

forming in solution which likely affected the kinetics of these experiments, as well as making the analysis of the data challenging, if not impossible by GC-FID.

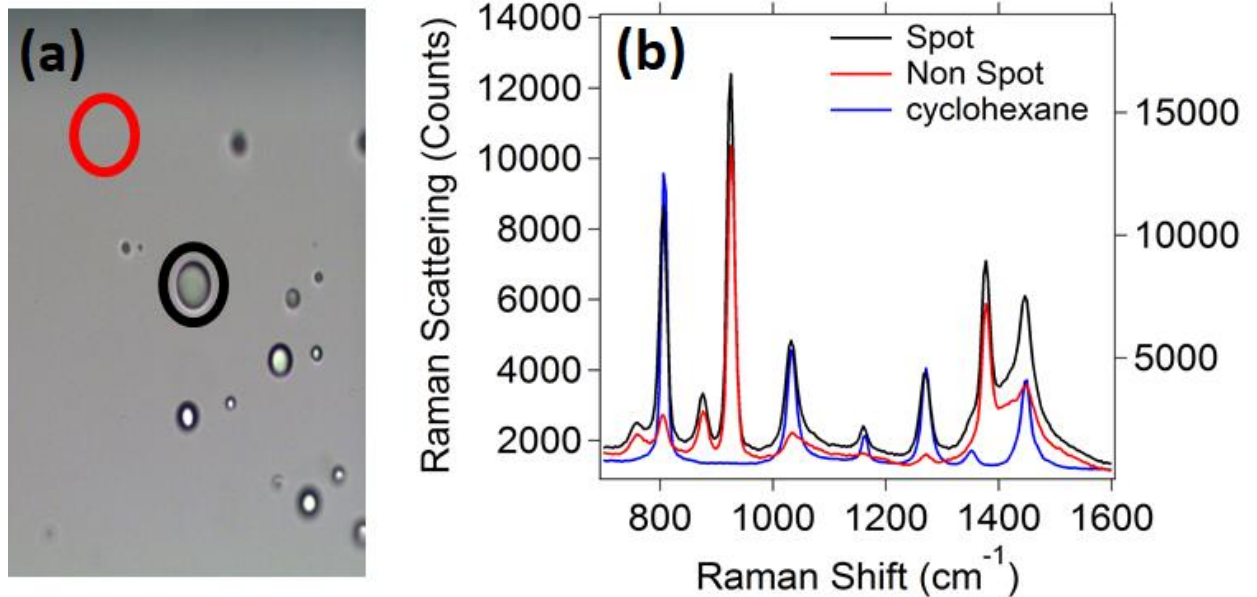


Figure 6. Raman Spectroscopic Data on Cyclohexane Oxidation. (a) Light microscopy (b) Raman spectra of described samples

The next step to further improve this method would involve a faster method of analysis. A typical experiment following the kinetics of 6 reactions over 24 hours can be 150 data points (if collected hourly). This amount of data can be cumbersome to workup. When deciphering the data by a typical GC method, this analysis takes 10-12 min per sample. Analysis on a full set of data can monopolize the GC continuously for over 36 consecutive hours. Some potential concepts for resolving these issues would be a redesign of the multi-well reactors to allow access points for fiber optic cables. Using

these fiber optic cables to perform in-situ IR or Raman spectroscopy could give real-time data resolving multiple peaks simultaneously.

Moving away from GC analysis would also help alleviate other issues which arose during analysis. As noted previously, a quenching agent (PPh_3) must be used to rapidly consume excess oxidant. As this quenching agent required stoichiometric quantities of material, the concentration of PPh_3 and OPPh_3 in solution was high. Typical GC analysis requires very low concentrations of analytes ($\sim 10\text{-}50$ ppm). Although the phosphine did not co-elute with our analytes, it did cause the plunger on the autosampler arm of the GC to freeze relatively often due to precipitated material in the syringe. It also caused problems with the splint-vent on the instrument, as the splint-vent line is not heated, so significant amounts of phosphine material condensed in the line clogged it completely. This can be a trivial fix but requires down-time on the instrument during maintenance which further increases the time for quantifying all samples.

The above described methodology has proven to be successful, although many adjustments were made over the course of these experiments to fully solve all the issues that arise. Expansion to new chemical reactions may prove easier, in situations where quenching is not necessary.

Introduction: Heterogeneous Catalyst Synthesis

Efficient upgrading of lignocellulosic biomass to essential commodity chemicals can have the impact of lowering anthropomorphic carbon footprint on the earth.

Developing new catalysts or finding easier ways of synthesizing efficient catalysts for

lignin depolymerization, and biomass upgrading can go a long way towards these goals. Heterogenous catalysts are used for a broad range of chemical transformations. Some of the advantages of heterogenous catalysts over homogeneous catalysts include the ease of separating the catalyst from the reaction mixture and the potential for catalyst recyclability. Reports of heterogeneous catalysts for lignin depolymerization and biomass upgrading are ubiquitous.²¹⁻²⁶ Our goal is to use an automated synthesis robot to prepare an array of solid supported catalytic materials.

Effectiveness of heterogeneous catalysts are governed by many properties, which include identity of support material, surface area of support material, catalyst loading and catalyst particle dispersion.²⁷ A common route to preparation of a heterogeneous catalyst is through the incipient-wetness method.^{28,29} This method involves dispensing a small volume of a concentrated solution of pre-catalyst to the support while grinding the mixture in a mortar and pestle. The solution is drawn into the pores of the material by capillary action. This is a slow, tedious process which requires physical labor. As the material properties may be influenced by mixing and grinding, often perfect replication of technique and therefore materials can be challenging. Making multiple materials for experimentation is laborious, time consuming and can suffer from human error during preparation.

An easier method of preparing these kinds of material could be designed in which larger volumes of dilute pre-catalyst solution are added over mixed supports as the solution is slowly evaporated in an iterative fashion (similar in scope to “wet impregnation”). Issues arise in which the pre-catalyst crystallizes out of the solution as it becomes more concentrated which potentially leads to poor catalyst dispersion and

inactive catalysts. Our goal is to utilize automation combined with high throughput experimentation to prepare libraries of heterogeneous catalyst materials, made in parallel, with high reproducibility. We hypothesize that iterative additions of dilute solutions with subsequent of evaporation steps will limit the large crystallization that occurs during a single addition of a more concentrated solution. This would be difficult to access conventionally, as it requires attention at frequent intervals over a long period of time (10-26 h).

Methods already exist to deposit heterogeneous catalysts on thin films using radio-frequency sputtering, to create a library of catalysts which have up to three metals deposited onto it. This involves iterative additions of 10 nm layers of material.³⁰ While this method is excellent for making a catalyst library for primary screening, it doesn't allow scale-up methods, which would require traditional catalyst preparation. Liquids have been added to thin films in similar iterative fashion using methods which include complexation, gelation, crystallization, ion exchange and grafting. Impregnation is the addition of a catalyst or pre-catalyst in solution to a porous solid which will either graft to the solid, or be calcined and activated on the surface of the material.

We assessed our goal by preparing a library of heterogeneous catalysts for lignin depolymerization. Our initial strategy involved identifying several supports and potential pre-catalysts, and synthesizing a small library of these materials. Catalyst loading was confirmed by inductively coupled plasma mass spectrometry (ICP-MS), and dispersion was calculated by chemisorption. We then used these prepared materials in experiments in high-pressure reactors to attempt to hydrogenate lignin model compounds.

Results and Discussion: Heterogeneous Catalyst Synthesis

We chose ceria (CeO_2), alumina (Al_2O_3), silica (SiO_2) and titania (TiO_2) as our target supports, and initially began to use $\text{Pd}(\text{OAc})_2$ 1% w/w Pd to support as our pre-catalyst. The typical procedure was to dissolve x mg of $\text{Pd}(\text{OAc})_2$ in acetone at the appropriate concentration for a 1% Pd addition by mass after n iterations. Solid supports were weighed out and placed into conical vials in an aluminum block while undergoing stirring from a magnetic stir bar. The Pd solution (0.9 mL) was dispensed into 0.5 g of support, after which, the block is moved into a reactor heated to 60°C to allow the solvent to slowly evaporate over 90 minutes. The block was then removed from the reactor into the solvent dispensing area, and the process was repeated over again. This iterative addition process was run comparing materials with 5-13 iterations.

After the Pd solutions were added, the materials were calcined in a box furnace and reduced in a tube furnace under flowing hydrogen. The materials were then analyzed by ICP-MS to determine the weight % Pd on the support and then analyzed by chemisorption to determine the % dispersion of the Pd on the support. The materials were then tested as hydrogenation catalysts, as they were used in hydrogenation experiments with guaiacol. Effectiveness of the catalyst was gauged based upon total conversion and cyclohexanol formation.

Investigation into SiO_2 materials began with iterative additions of $\text{Pd}(\text{OAc})_2$ solution into the stirred supports. ICP measurements demonstrated consistent amounts of Pd being deposited on the surface on materials made with 5-12 iterations (Table 2). Interestingly, dispersion and iterations did not show strong correlation. The conical vial and stir bar was necessary for optimal material preparation. Experiments performed in a

20-mL scintillation vial without a stir-bar had poor catalyst loading and dispersion (Table 2, Entry 4). After treatment, significant amounts of Pd(OAc)₂ precipitate was observed on the walls of the vial.

Table 2. Catalyst Loading and Dispersion of Pd on SiO₂ Support

Entry	Iterations ^a	Pd w/w% ^b	Dispersion (%) ^c	Dispersion (%) (ICP) ^d
1	5	0.71 (0.012)	77.7	97.1
2	7	0.78 (0.037)	83.2	104.1
3	11	0.74 (0.012)	83	103.7
4	11 ^e	0.74 (0.042)	19.2	27.5
5	12	0.7 (0.028)	69.7	87.1

^a Number of catalyst solution addition/evaporation steps. ^b Calculated by ICP-MS. ^c

Dispersion calculated based on 1 w/w% Pd on support. ^d Dispersion calculated based on Pd loading as calculated from ICP-MS measurements. ^e Material vortexed while evaporating solvent in absence of stir-bar in a 20-mL glass scintillation vial.

Investigation into the Al₂O₃ materials gave similar results as the SiO₂ materials (Table 3). Pd amounts were consistent between iterations as calculated by ICP-MS. Unlike with SiO₂, materials prepared in 11 or 12 iterations had significantly higher dispersion versus materials prepared with only 5 or 7 iterations. As with SiO₂ materials, experiments performed in a 20-mL scintillation vial without a stir-bar had poor catalyst

loading and dispersion (Table 3, Entry 4). This indicates that the shape of the vial and method of mixing was important to the overall quality of the material.

Table 3. Catalyst Loading and Dispersion of Pd on Al₂O₃ Support

Entry	Iterations ^a	Pd w/w% ^b	Dispersion (%) ^c	Dispersion (%) (ICP) ^d
1	5	0.83 (0.014)	57.9	69.7
2	7	0.84 (0.014)	24.3	28.9
3	11	0.76 (0.040)	93.8	109.1
4	11 ^e	0.81 (0.010)	19.3	24.1
5	12	0.81 (0.024)	88.3	101.2

^a Number of catalyst solution addition/evaporation steps. ^b Calculated by ICP-MS. ^c

Dispersion calculated based on 1 w/w% Pd on support. ^d Dispersion calculated based on Pd loading as calculated from ICP-MS measurements. ^e Material vortexed while evaporating solvent in absence of stir-bar in a 20-mL glass scintillation vial.

Investigations into the CeO₂ materials gave interesting results in comparison to the TiO₂ materials (Table 4). There was poor Pd concentration compared to other tested supports, and dispersion was similarly poor. Upon close visual observation of the solvent additions, some of the commercial supports did not stir consistently. The densities and granularities of the supports varied, and this attributed to the consistency of the Al₂O₃, and inconsistency of both CeO₂ and SiO₂. Neither of the latter materials had the uniform stirring of the Al₂O₃ and this likely attributed to the data.

Table 4. Catalyst Loading and Dispersion of Pd on CeO₂ Support

Entry	Iterations ^a	Pd w/w% ^b	Dispersion (%) ^c	Dispersion (%) (ICP) ^d
1	11	0.63 (0.007)	50.7	72.1
2	12	0.81 (0.076)	35.8	82.2
3	13	0.66 (0.007)	39.6	56.5

^a Number of solvent addition/evaporation steps. ^b Calculated by ICP-MS. ^c Dispersion calculated based on 1 w/w% Pd on support. ^d Dispersion calculated based on Pd loading as calculated from ICP-MS measurements.

A series of hydrogenolysis experiments were performed using some of the prepared materials. Reactions using SiO₂ supported catalysts had poor-moderate conversion (14.7-16.0%), as well as poor-moderate selectivity for cyclohexanol (14.7-15.4%) (Table 5, Entries 1 and 2). TiO₂ supported catalysts (which have yet to be analyzed by ICP-MS and Chemisorption) had similarly poor-moderate conversion (17.6-20.9%) and selectivity (6.7-13.0%) (Table 5, Entries 3 and 4). High dispersion Pd on alumina had some of the best results for the conversion of guaiacol (Table 5, Entries 5 and 6). The catalyst prepared with 12 iterations had 69.4% conversion while the material prepared with only 5 iterations had 52.2% conversion. Selectivity for conversion to cyclohexanol followed a similar trend with 25.4% selectivity versus 21.2% for the material prepared with fewer iterations. CeO₂ supported catalysts gave somewhat surprising results, conversion of guaiacol was similar between two of the test iterations (18.3 vs 20.1% conversion, Table 5, Entries 7 and 8), but as selectivity for cyclohexanol was 24.4% in the material prepared with 5 iterations, no cyclohexanol was formed in the material prepared with 13 iterations. All the materials discussed above were prepared on

commercial grade supports. Hui Zhou prepared CeO₂ following the previously reported procedure by Nicholas Nelson.³¹ Pd(OAc)₂ was added to this bespoke material over 13 iterations. Under hydrogenolysis conditions, this material underwent full conversion of guaiacol, producing cyclohexanol with excellent (62.5%) selectivity (Table 5, Entry 9). Physically, the bespoke ceria was significantly denser than the commercial grade material. As noted above, during additions of Pd(OAc)₂, there was difficulty with mixing some of the materials. Commercial CeO₂ in particular, was not able to be mixed consistently, if at all. The lab-made CeO₂ was both more dense and granular allowing for much more efficient mixing, which likely contributed to the increased catalytic response.

Table 5. Prepared materials as Catalysts for Guaiacol Hydrogenolysis

Material	Entry	Iterations ^a	Guaiacol	Cyclohexanol
			Conversion (%) ^b	Selectivity (%) ^b
SiO ₂	1	5	14.7	15.4
	2	13	16.0	14.7
TiO ₂	3	5	20.9	6.7
	4	12	17.6	13.0
Al ₂ O ₃	5	5	52.2	21.2
	6	12	69.4	25.4
CeO ₂	7	5	20.1	24.4
	8	13	18.3	0
	9	13 ^c	100	62.5

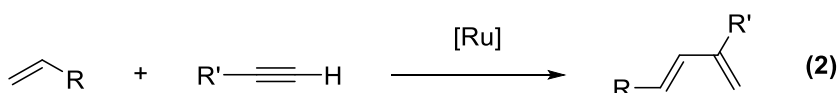
^a Number of catalyst solution addition/evaporation steps. ^b Calculated by GC-MS. ^c CeO₂ support prepared by Hui Zhou (non-commercial material)

The results of this initial work indicate that this strategy of iterative additions of catalyst solution to support materials can perhaps be a new method of preparing catalytic materials. To increase success, there are still several areas on which to improve. As discussed above, some materials are difficult to stir (commercial SiO_2 and CeO_2). Lab made materials which are prepared with bespoke properties to achieve a better free flowing granular solid can help improve that. A more optimized reaction flask with a well-fit stir bar can likely help to achieve the same goals. Alternative needles for syringing are available as well, which allow for the solution to be dispensed in a spray, as opposed to the dropwise addition from a needle that is currently in place. As the technology improves, it is feasible to imagine adding solution over solid that is even being vortexed to further improve mixing.

Introduction: Enyne Metathesis

Functionalized polymers are defined as polymers or macromolecules which are chemically bound to an external functional group, often these are prepared by modification of the end chain of a polymer. These functionalized have several advantages which include ease of separation, synthesis of cross-linked polymers, or even binding an expensive or rare material to a polymer. Some of the drawbacks include the difficulty to functionalize polymers, by time and/or cost and potentially slower polymerizations with poor yield.³²

Another potential method toward polymer functionalization could involve functionalizing monomers prior to bulk polymerization. Bradley Schmidt began to study enyne metathesis as a strategy for synthesizing functionalized monomers (Eq. 2). Ruthenium catalysts have been used as a strategy for end-functionalized polymers,³³ and commonly used as a metathesis catalyst for synthesizing butadiene derivatives.³⁴⁻³⁶



Results and Discussion: Enyne Metathesis

The PD reactors in the Chemspeed Swing-XL allow for design of intricate experiments in sealed reactors. These experiments would typically prove impossible using conventional Schlenk glassware. The 6 PD reactors each include a high-pressure pump, which allows for dispensing of liquids into the reactors while being heated and under pressure and allows for sampling of reaction solution. The reactors are extensively modifiable, allowing for pressure to be controlled by regulator or mass flow controller. The reactor head also includes multiple Swagelok ports, which allow for installation of a dip tube with a ball valve for sampling, or other potential additions like pH probe.

Conventional Schlenk chemistry restricted these reactions to the limitations of a Fisher-Porter vessel. The PD reactors had a pressure rating roughly 10x higher than the Fisher-Porter vessel and allowed accurate control over internal reactor temperature and stir rate. The effect of increased ethylene pressure was immediately realized as a form of increased catalyst turnovers. Further studies indicated that the metathesis catalyst has a

very short lifespan. Using the high-pressure pumps, we can add catalyst slowly, after all substrates are placed in the sealed reactor after it begins to heat under pressure. Once under the described reaction conditions, a catalyst solution can be slowly pumped into the reactor, which gives a large increase in conversion by having a continuous source of catalyst over the course of addition. We quantified the reaction by turnovers of catalyst (**Table 6**) and found that higher pressures of ethylene enhanced the reaction, and the catalyst performed best when it was added slowly to a heated, pressurized reactor.

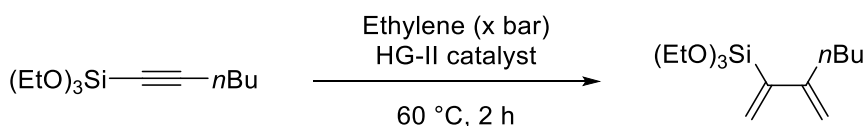


Table 6. Comparison of Different Reactors for Enyne Metathesis.

Ethylene (bar)	TON
1.5 ^a	80
40 ^b	20
40 ^c	200

Conditions: 60 °C, 2 h. ^a All substrates added prior to gas addition in high pressure NMR tube (0.2 mol% HG-II catalyst) ^b All substrates added prior to gas addition in Parr reactor (1.0 mol% HG-II catalyst) ^c Reactor pressurized with ethylene (40 bar) and heated prior to slow addition of catalyst through high-pressure pumps (0.1 mol% HG-II catalyst)

While some synthesis robots are built into an air-free glovebox, our instrument converts between air and air-free conditions. When required for air-free techniques,

significant care must be taken to remove air and moisture from the robot, all the plumbing lines, as well as individual reactors. For the large volume of the box, N₂ can be pumped in to displace air. Individual reactors can be heated under vacuum and purged with N₂. The solvent lines in the high-pressure pump have a very small inner diameter (1/32") and therefore require substantial volumes of anhydrous solvent to flush out "wet solvent" prior to introduction of the catalyst solution.

As the instrument is incredibly complex, we experienced critical errors, some of which were difficult to resolve. Each PD reactor has over two dozen connections, each of which could leak gas, allow for solvent evaporation, and ruin the reproducibility of the experiment. These issues were easy to identify and easy to correct. However, as the gas delivery was controlled through solenoids, critical failures in the solenoid were spontaneous and unresolvable. We attempted to mitigate these issues by pressurizing with reactive gas and venting prior to introducing reagents to the system.

Conclusion

Although it allows for a variety of bespoke experiments with novel utilization, an instrument as complicated as the Swing-XL has some significant drawbacks. Potentially the hardest challenge to overcome is the large upfront cost. Continuous costs will occur from typical chemical consumables (solvents, vials, o-rings, septa, solenoids etc.) but also from instrument servicing. In the event of breaking or failure of a peripheral, specialized new parts need to be ordered, potentially requiring an in-house visit for installation of the new/replaced peripheral. This downtime can lead to valuable lost productivity on the

instrument. Finally, as the instrument is extensively complex, there is a steep learning curve to successful use of the instrument which can overwhelm new users.

Even with these drawbacks, the potential for reaching new, unrealized goals is expanded using new technology. We successfully developed methods for studying the kinetics of several experiments simultaneously. This work is currently being expanded to other experiments, in hope that the analysis can eventually become fully automated, and potentially even expanded into a machine learning type environment. Many of the problems which occurred in these oxidation reactions can easily be resolved by using a different reaction system. Use of a new analytical technique to study the kinetics can also be used to study a vast landscape of chemical transformations. In the synthesis of heterogeneous catalysts, we quickly determined what the limitations of the system is. We have hypothesized new methods of resolving this through external stirring, or even preparing these materials on a larger scale in the PD reactors. The strategy of iterative addition of catalyst solutions has shown viability, especially with the lab-prepared CeO_2 for hydrogenolysis reactions. Finally, we utilized the specialized PD reactors for optimizing enyne metathesis reactions. A lot of work was required to get these reactors to work at their most optimal capabilities, but now intricate reactions can be performed in which reagents are fed in during reactions, and samples can be pumped out through the same methods.

Experimental

General procedure for High-Throughput Kinetics (As written for $\text{To}^{\text{M}}\text{CoOAc}$)²⁰

A reaction flask was charged with cyclohexane (1.6 mL, 15 mmol, 2.45 M) and $\text{To}^{\text{M}}\text{CoOAc}$ (1 μmol , 0.16 mM) dissolved in dichloromethane/acetonitrile (95 %, 1 mL). Upon the addition of 1,2-dichloroethane/acetonitrile (3.5 mL, 97.5 %) containing mCPBA (345 mg, 2.0 mmol) and nitrobenzene (30 μL , 300 μmol), the reaction was initiated and maintained at 25 °C. At each time point, an aliquot (0.2 mL) was removed and quenched with triphenylphosphine (10 mg, 38.1 μmol). The organic products were identified and quantified by GC–MS through the integration of the peak areas with respect to a known amount of the nitrobenzene standard. In this analysis, the quenched reaction product (10 μL) was added to dichloromethane (1.5 mL) and analyzed by GC–MS. Each chromatogram was obtained under the following conditions: split, 25:1; inlet temperature, 250 °C; initial oven temperature, 45 °C; temperature ramp, 15 °C min^{-1} to 150 °C. From this data, the concentration of cyclohexanol versus time was analyzed with a nonlinear least-squares regression.

General Procedure for Heterogeneous Catalyst Synthesis (For a catalyst prepared in 13 iterations)

Solid catalyst support (0.5 g) was weighed out into a conical reaction vial equipped with a stir bar. $\text{Pd}(\text{OAc})_2$ in acetone was added dropwise over stirring catalyst (0.9 mL, 4.0 mM). The vial array was moved into a reactor heated to 60 °C as the solvent was left to

evaporate for 90 minutes. The vial array was replaced over the stir plate, and the addition of solvent and evaporation were repeated a total of 13 times.

The material was calcined in a box furnace at 300 °C for 2 h. (Ramp rate 20 to 300 °C, 2 °C/min). It was then allowed to reduce in a tube furnace under flowing H₂ at 300 °C for 2 h. (Ramp rate 20 to 300 °C, 2 °C/min). The materials were then tested for metal loading via ICP-MS and metal dispersion via chemisorption.

References

- (1) Manzano, J. S.; Weinstein, Z. B.; Sadow, A. D.; Slowing, I. I. *ACS Catal.* **2017**, *7* (11), 7567–7577.
- (2) Symes, M. D.; Kitson, P. J.; Yan, J.; Richmond, C. J.; Cooper, G. J. T.; Bowman, R. W.; Vilbrandt, T.; Cronin, L. *Nat. Chem.* **2012**, *4* (5), 349–354.
- (3) Kitson, P. J.; Symes, M. D.; Dragone, V.; Cronin, L. *Chem. Sci.* **2013**, *4* (8), 3099–3103.
- (4) Harper, K. C.; Bess, E. N.; Sigman, M. S. *Nat. Chem.* **2012**, *4* (5), 366–374.
- (5) Bess, E. N.; Bischoff, A. J.; Sigman, M. S. *Proc. Natl. Acad. Sci.* **2014**, *111* (41), 14698–14703.
- (6) Milo, A.; Neel, A. J.; Toste, F. D.; Sigman, M. S. *Science* **2015**, *347* (6223), 737–743.
- (7) Shevlin, M. *ACS Med. Chem. Lett.* **2017**, *8* (6), 601–607.

- (8) Fedorov, A.; Liu, H. J.; Lo, H. K.; Copéret, C. *J. Am. Chem. Soc.* **2016**, *138* (50), 16502–16507.
- (9) Troshin, K.; Hartwig, J. F. *Science* **2017**, *357* (6347), 175–181.
- (10) Engl, P. S.; Santiago, C. B.; Gordon, C. P.; Liao, W. C.; Fedorov, A.; Copéret, C.; Sigman, M. S.; Togni, A. *J. Am. Chem. Soc.* **2017**, *139* (37), 13117–13125.
- (11) Molander, G. A.; Wisniewski, S. R. *J. Am. Chem. Soc.* **2012**, *134* (40), 16856–16868.
- (12) Molander, G. A.; Cavalcanti, L. N.; García-García, C. *J. Org. Chem.* **2013**, *78* (13), 6427–6439.
- (13) Dreher, S. D.; Dormer, P. G.; Sandrock, D. L.; Molander, G. A. *Org. Synth.* **2008**, 9257–9259.
- (14) Metz, A. E.; Berritt, S.; Dreher, S. D.; Kozlowski, M. C. *Org. Lett.* **2012**, *14* (3), 760–763.
- (15) Bellomo, A.; Celebi-Olcum, N.; Bu, X.; Rivera, N.; Ruck, R. T.; Welch, C. J.; Houk, K. N.; Dreher, S. D. *Angew. Chem. Int. Ed.* **2012**, *51* (28), 6912–6915.
- (16) Newhouse, T.; Baran, P. S. *Angew. Chem. Int. Ed.* **2011**, *50* (15), 3362–3374.
- (17) Tomás, R. A. F.; Bordado, J. C. M.; Gomes, J. F. P. *Chem. Rev.* **2013**, *113* (10), 7421–7469.
- (18) Nakazawa, J.; Yata, A.; Hori, T.; Stack, T. D. P.; Naruta, Y.; Hikichi, S. *Chem. Lett.* **2013**, *42* (10), 1197–1199.

- (19) Schuchardt, U.; Cardoso, D.; Sercheli, R.; Pereira, R.; Da Cruz, R. S.; Guerreiro, M. C.; Mandelli, D.; Spinacé, E. V.; Pires, E. L. *Appl. Catal. A Gen.* **2001**, *211* (1), 1–17.
- (20) Reinig, R. R.; Mukherjee, D.; Weinstein, Z. B.; Xie, W.; Albright, T.; Baird, B.; Gray, T. S.; Ellern, A.; Miller, G. J.; Winter, A. H.; Bud'ko, S. L.; Sadow, A. D. *Eur. J. Inorg. Chem.* **2016**, *2016* (15–16), 2486–2494.
- (21) Sturgeon, M. R.; O'Brien, M. H.; Ciesielski, P. N.; Katahira, R.; Kruger, J. S.; Chmely, S. C.; Hamlin, J.; Lawrence, K.; Hunsinger, G. B.; Foust, T. D.; Baldwin, R. M.; Bidy, M. J.; Beckham, G. T. *Green Chem.* **2014**, *16* (2), 824–835.
- (22) Pineda, A.; Lee, A. F. *Appl. Petrochemical Res.* **2016**, *6* (3), 243–256.
- (23) Espro, C.; Gumina, B.; Paone, E.; Mauriello, F. *Catalysts* **2017**, *7* (3), 78.
- (24) Luo, H.; Abu-Omar, M. M. *Green Chem.* **2018**.
- (25) Gilkey, M. J.; Xu, B. *ACS Catal.* **2016**, *6* (3), 1420–1436.
- (26) Wabeke, J. T.; Al-Zubaidi, H.; Adams, C. P.; Ariyadasa, L. A. W.; Nick, S. T.; Bolandi, A.; Ofoli, R. Y.; Obare, S. O. In *Green Technologies for the Environment*; ACS Symposium Series; American Chemical Society, 2014; Vol. 1186, pp 12–219.
- (27) Prieto, G.; Zečević, J.; Friedrich, H.; De Jong, K. P.; De Jongh, P. E. *Nat. Mater.* **2013**, *12* (1), 34–39.
- (28) Schwarz, J. A.; Contescu, C.; Contescu, A. *Chem. Rev.* **1995**, *95* (3), 477–510.
- (29) Munnik, P.; De Jongh, P. E.; De Jong, K. P. *Chem. Rev.* **2015**, *115* (14), 6687–

6718.

- (30) Potyrailo, R.; Maier, W.; Czarnik, A.; Yan, B.; Webster, D.; Schunk, S.; Svedberg, E.; Gao, C.; Woo, D.; Alexanian, A.; Al., E. *Combinatorial and High-Throughput Discovery and Optimization of Catalysts*; Shinar, J., Ed.; CRC Press: Boca Raton, 2006.
- (31) Nelson, N. C.; Manzano, J. S.; Sadow, A. D.; Overbury, S. H.; Slowing, I. I. *ACS Catal.* **2015**, *5* (4), 2051–2061.
- (32) Akelah, A.; Sherrington, D. C. *Chem. Rev.* **1981**, *81* (6), 557–587.
- (33) Hillmyer, M. A.; Nguyen, S. B. T.; Grubbs, R. H. *Macromolecules* **1997**, *30* (4), 718–721.
- (34) Clark, D. A.; Basile, B. S.; Karnofel, W. S.; Diver, S. T. *Org. Lett.* **2008**, *10* (21), 4927–4929.
- (35) Griffiths, J. R.; Keister, J. B.; Diver, S. T. *J. Am. Chem. Soc.* **2016**, *138* (16), 5380–5391.
- (36) Marshall, J. E.; Keister, J. B.; Diver, S. T. *Organometallics* **2011**, *30* (6), 1319–1321.

Supporting Information

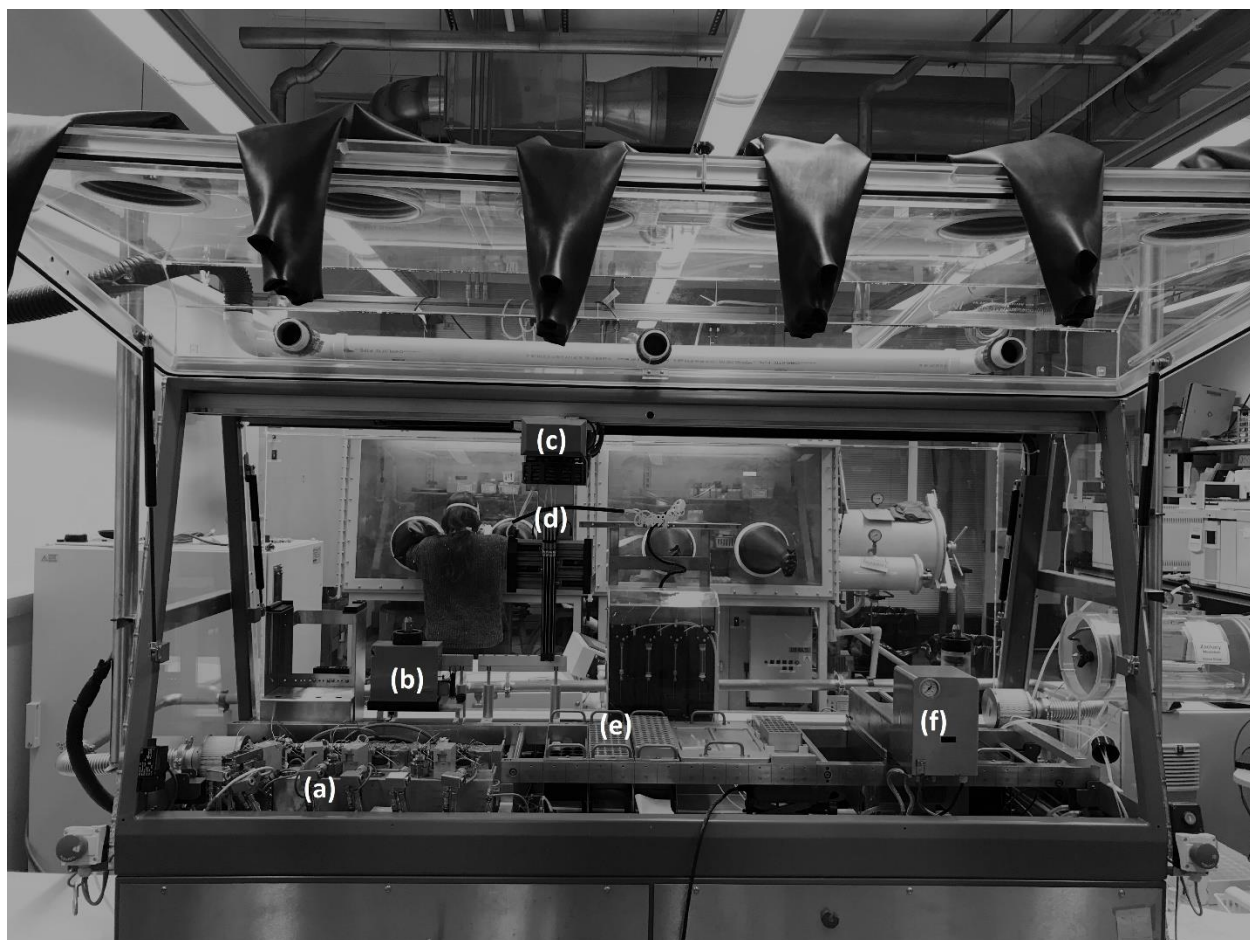


Figure S1. Chemspeed SWING-XL Automated Synthesis Platform. ^a PD Reactor array
^b Gravimetric balance ^c XYZ α arm ^d 4-needle head solvent dispensing system ^e Sampling
station ^f MTP reactor

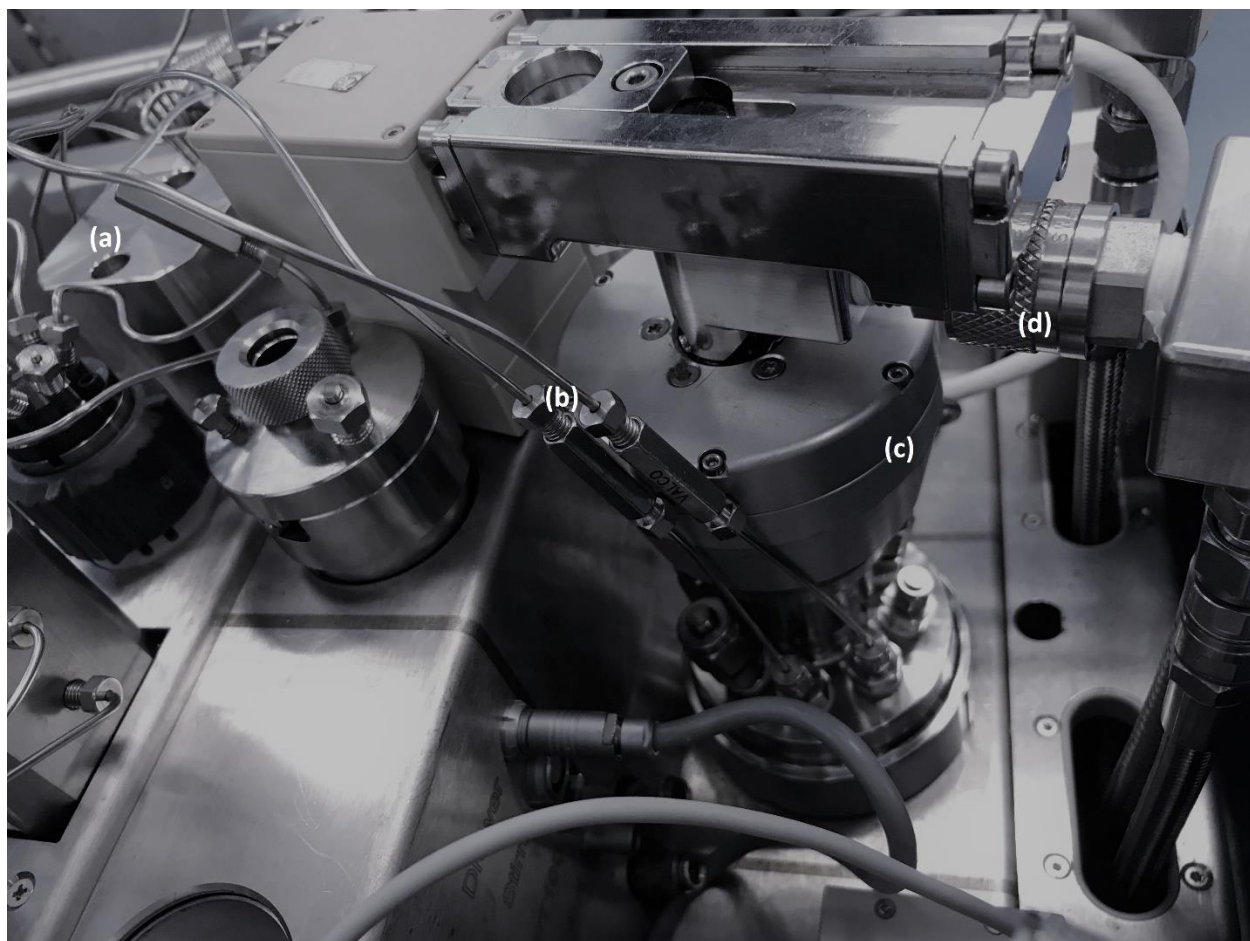


Figure S2. Close-up image of Chemspeed SWING-XL PD Reactor. ^a High pressure pump ^b High pressure feed line ^c Stirrer motor ^d High pressure gas line



Figure S3. Close-up image of Chemspeed SWING-XL MTP Block. ^a 4-needle head solvent dispensing system ^b MTP block vial racks ^c MTP block reactor ^d Gripper tool

**CHAPTER 4. INVESTIGATION OF [XANTPHOSRH(COD)]BAR^F FOR
CATALYTIC REDUCTION OF SECONDARY AND TERTIARY AMIDES BY
PHENYLSILANE**

Modified from a paper to be submitted to a journal

Zachary B. Weinstein, Dr. Aaron D. Sadow*

Abstract

The cationic Rh(I) species [XantphosRh(cod)]BAR^F (**1**) (cod = 1,5-cycloocatadiene; BAR^F = Tetrakis[3,5-bis(trifluoromethyl)phenyl]borate) was demonstrated to catalyze the reduction of a series of secondary and tertiary amides to amines using phenylsilane as a reductant. This system requires low catalyst loading (1 mol %), requires mild reaction conditions (25 – 60 °C) and short reaction times with adequate functional group tolerance. Reactions of tertiary amides occur readily with 2 equiv. of phenylsilane, while secondary amides require 10 equiv. of phenylsilane. **1** also demonstrated an affinity for catalytic disproportionation of phenylsilane which generated hydrogen gas in-situ.

Introduction

Amines are one of the most important classes of compounds, being used extensively in the pharmaceutical industry as in the synthesis of more complex molecules.¹ As direct synthesis of amines can be difficult, reduction of amides are a

common method for synthesizing amines.^{2,3,4} Amide reductions traditionally require stoichiometric equivalents of a hydride reagent such as lithium aluminum hydride (LiAlH_4). The harsh conditions, air and water sensitivity, poor functional group tolerance and large quantities of salt byproducts such as lithium aluminum hydroxide make these reactions less favorable on an industrial scale. Regardless of the drawbacks, LiAlH_4 continues to be used industrially.⁵

Late metal catalyzed reductions of tertiary amides are well established, evidenced by $\text{RhH}(\text{CO})(\text{PPh}_3)$ catalyzed reductions with Ph_2SiH_2 as a reductant.⁶ Cationic Ir species have shown selectivity for reducing tertiary amides,⁷ while secondary amides has been reported to be reduced with commercially available $[\text{IrCl}(\text{cod})]_2$ as a catalyst.⁸ These Ir catalysts were both appreciably more efficient as catalysts versus the earlier reported Rh species. Most reported systems typically catalyze the reduction secondary or tertiary amides. The platinum species $\text{H}_2\text{PtCl}_6 \cdot 6\text{H}_2\text{O}$ ⁹ was reported to reduce both tertiary and secondary amides with polymethylhydrosiloxane, (PMHS) which can be a safer alternative to other hydrosilanes.¹⁰ The near limitless use of catalysts utilizing hydrosilanes reducing amides include but are not limited to iron,¹¹ platinum,¹² titanium¹³ and boronic acids.¹⁴

Xantphos is a well-defined,¹⁵ commercially available ligand which has been used with Rh for a variety of catalytic reactions. Xantphos and $[\text{RhCl}(\text{cod})]_2$ has been used as a catalyst for borylation of nitriles.¹⁶ Xantphos and $[\text{Rh}(\text{CO})_2(\text{acac})]$ has been used as a hydroformylation catalyst,¹⁷ as well as a catalyst for methanol oxidation.¹⁸ Cationic $[\text{XantphosRh}]^+$ complexes have also been used extensively in general catalysis^{19,20} and their reactivity with hydrosilanes has been well documented.^{21,22} Here we report the use

of [XantphosRh(cod)]BAR^F (**1**) for the catalytic reduction of tertiary and secondary amides, and document our study of the reactivity of **1** with hydrosilanes.

Results and Discussion

We began investigating group 9 metal rhodium and iridium complexes (Table 1) as these late metals are highly effective for hydrosilylation reactions as discussed above. [RhCl(cod)]₂ catalyzes the reduction of dibenzylbenzamide by phenylsilane to tribenzylamine in 57% yield, while the Ir analog [Ir(cod)Cl]₂ catalyzes the same reaction in 19% yield. XantphosRh(cod)Cl²³ acts as a marginally better catalyst (vs. [RhCl(cod)]₂) increasing yields of tribenzylamine to 61%. The use of cationic [XantphosRh(cod)]⁺ species (via NaBAR^F or AgBF₄) as a catalyst increases yield of tribenzylamine to 97 and 94% yield respectively. Cationic Ir complexes also are more efficient than their neutral counterparts.

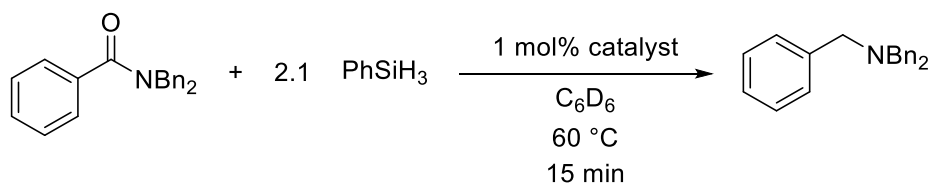


Table 1. Catalyst screening of dibenzylbenzamide reduction

Catalyst	Yield (%) ^a
[RhCl(cod)] ₂	57.1
XantphosRh(cod)Cl	61.6
XantphosRh(cod)BAR ^F (1)	96.6

Table 1. (continued)

XantphosRh(cod)BF ₄	93.9
[IrCl(cod)] ₂	19.3
XantphosIr(cod)BAr ^F	43.5
XantphosIr(cod)BF ₄	65 ^b

Conditions: N,N-dibenzylbenzamide (0.1 mmol), phenylsilane (0.21 mmol) and catalyst (0.001 mmol) in benzene-*d*₆ at 60 °C for 15 min. ^a Yield calculated by ¹H NMR. ^b Heated at 60 °C for 60 min.

Next, we began to investigate the influence of silane in the reduction of tertiary amides catalyzed by **1** (Table 2). Identity of silane played a very large role in yield of amine. Primary silanes such as phenylsilane gives higher yields of tribenzylamine (58%) tested reaction conditions versus secondary and tertiary silanes. Only starting material was observed in reactions in which simple tertiary silanes such as benzyldimethylsilane or triethylsilane were used. Reactions with polymeric tertiary silane polymethyl hydrosiloxane (PMHS) yields a trace amount of amine product. Reactions with tetramethyldisiloxane (TMDS) have relatively low yield of tribenzylamine (14%). Reactions using secondary silanes, benzyldimethylsilane and diphenylsilane, have moderate yields of tribenzylamine (33 and 8% respectively), while reactions using the primary silanes, phenylsilane and *n*-hexylsilane, have the highest yields of tribenzylamine (58 and 75% respectively) of all silanes tested. Although reactions with *n*-hexylsilane had higher yields than that of phenylsilane, we proceeded to use phenylsilane as the reductant due to issues that arise when using *n*-hexylsilane is employed as a reductant for

secondary amides (to be discussed later). The difference between the yield of tribenzylamine with phenylsilane between Table 1 and Table 2 can be attributed to the difference in concentration of reactants.

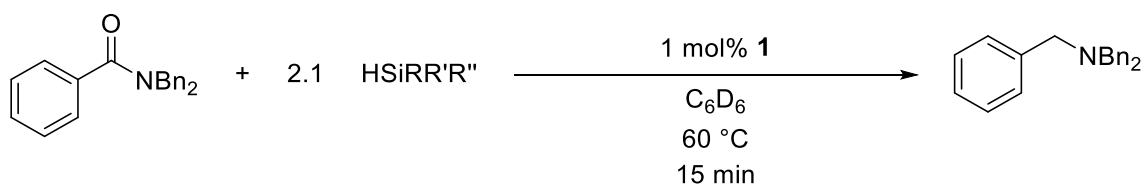


Table 2. Silane screening of dibenzylbenzamide reduction

Silane	Yield (%) ^a
PhSiH ₃	58
Ph ₂ SiH ₂	8
TMDS	14
Et ₃ SiH	0
PhCH ₃ SiH ₂	33
Bn(CH ₃) ₂ SiH	0
<i>n</i> -CH ₃ (CH ₂) ₅ SiH ₃	75
PMHS	trace

Conditions: N,N-dibenzylbenzamide (0.05 mmol), silane (0.11 mmol) and **1** (0.005 mmol) in benzene-*d*₆ at 60 °C for 15 min. ^a Yield calculated by ¹H NMR.

Applying these optimized conditions using **1** as a catalyst with PhSiH₃ was applied to a series of tertiary amides, producing their corresponding amines. For easier

workup, all scaled up reactions were isolated as an amine HCl salt, by adding ethereal HCl to the reaction mixture precipitating out the product. During our substrate screen (Table 3), we found several amides which reacted very fast at room temperature (Entries 1-3) that consisted of a formamide, benzamide and acetamide. Most of the other amides tested reacted readily at 60 °C, with reasonable functional group tolerance. Bulkier substituents such as pivalamides and N-heterocyclic amides also reacted in good yield with the exception of dibenzylpivalamide (20% yield, Entry 6). Amides containing *p*-chloro or *p*-fluorobenzamides also yielded their reduced amine counterparts in excellent yield (Entries 12-13), however they required much longer reaction times (18 h). Amides containing alkene moieties were also tested, (Entry 14, 15) but required purging nitrogen to remove hydrogen, for reasons which will be discussed later. Amides containing nitro-substituents were tested as well, but the nitro- group was shown to be reduced to the primary amine counterpart.

Table 3. XantphosRh(cod)Bar^F Catalyzed Reduction of Tertiary Amides

entry	amide	time (min)	yield (%) ^d	entry	amide	time (min)	yield (%) ^d
1 ^a		15	87	8 ^b		10	98
2 ^a		30	81	9 ^b		10	62
3 ^a		5	64	10 ^b		20	84
4 ^b		15	96	11 ^b		10	62
5 ^b		30	76	12 ^b		18 h	86
6 ^b		5	20	13 ^b		18 h	90
7 ^b		5	93	14 ^c		120	90
				15 ^c		120	80

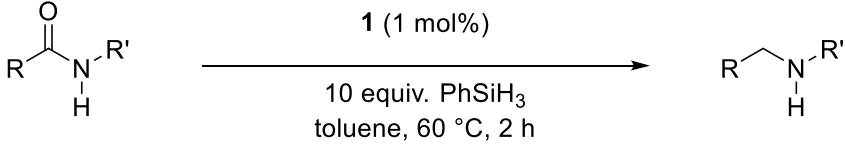
^a Run at room temperature ^b Run at 60 °C ^c Run at 60 °C under flowing N₂ ^d Reported

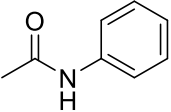
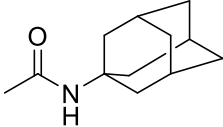
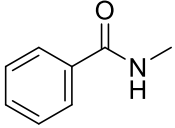
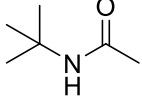
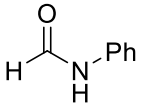
yields are isolated yield of HCl amine salt

XantphosRh(cod)BAr^F was also shown to be able to catalyze reduction of secondary amides. However, under the same conditions as tertiary amide reduction, reactions of secondary amides form multiple products. The reaction of N-phenylformamide and 2 equiv. PhSiH₃ in the presence of catalytic XantphosRh(cod)BAr^F yields N-methylaniline, aniline, dimethylaniline and N-phenylmethanimine. Analogous results are observed when other secondary amides are tested. This disproportionation of the amine is unwanted, but can be resolved by using excess quantities of silane. Increasing phenylsilane from 2 to 10 equivalents inhibits side product formation and yields exclusively secondary amines. Likely this occurs by protecting the amide via dehydrocoupling of the N-H bond with hydrosilanes. Phenylsilane is the most effective silane tested for selective reduction of secondary amides. While *n*-hexylsilane appears to be slightly more active in some tertiary amides, side-products of primary and tertiary amines were observed even with 10 equivalents of silane.

A brief investigation into the reduction of primary amides was also tested. Acetamide and benzamide were tested as substrates using similar conditions to the reduction of both secondary and tertiary amides, however the primary amide did not undergo conversion. Increasing the equivalents of silane, or increasing the reaction temperature up to 120 °C did not cause any conversion either. We concluded that this system would not be effective for primary amide reduction.

Table 4. XantphosRh(cod)Bar^F Catalyzed Reduction of Secondary Amides



entry	amide	yield (%) ^a	entry	amide	yield (%) ^a
16		94	19		69
17		90	20		38
18		91			

^a Reported yields are isolated yield of HCl amine salt

Over the course of these experiments, **1** was identified as being only slightly soluble in benzene, but fully dissolves after the addition of hydrosilanes. In C₆D₆, three doublets were observed by ³¹P NMR, (12.36, 21.06, 33.94 ppm; 144, 121, 120 Hz respectively) indicating multiple species in solution. After the addition of phenylsilane, the catalyst becomes fully soluble in benzene, but the identity of the active species could not be determined due to the broadening of the peaks in ³¹P over a very large range. **1** is much more soluble in more polar solvents such as methylene chloride, and in CD₂Cl₂, we

observe only two doublets by ^{31}P NMR, (12.40, 21.10 ppm; 144, 139 Hz), while XantphosRh(cod)Cl only has one doublet at 8.47 ppm (138 Hz).

In most of these reactions, a species was observed in GCMS and ^1H NMR, with a molecular weight of 151 and a ^1H NMR shift of 5.32 ppm, indicating the siloxane species which formed, 1,3-diphenyldisiloxane, which is a potential side product formed in this reaction. In the presence of excess (10 equiv.) silane, both the silane and siloxane are observed.

Over the course of these reactions, PhSiH_3 slowly disproportionates to Ph_2SiH_2 and trace amounts of Ph_3SiH (Table 5). Disproportionation or redistribution of primary or secondary hydrosilanes is not unprecedented. It has been reported to occur in the presence of Wilkinson's catalyst.^{24,25} At the end of the catalysis, disproportionation occurs much more rapidly, generating hydrogen and secondary and tertiary hydrosilanes. It is this gradual generation of hydrogen which acts to reduce amido-olefins and amino-olefins, requiring some reactions to be performed under flowing N_2 to drive off the generated hydrogen gas.

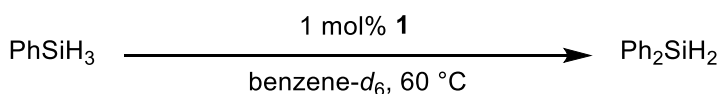


Table 5. Conversion of PhSiH_3 and yield of Ph_2SiH_2 Catalyzed by **1**

Time (h)	Conversion of PhSiH_3 (%) ^a	Yield of Ph_2SiH_2 (%) ^a
0.2	25	10
1	45	18

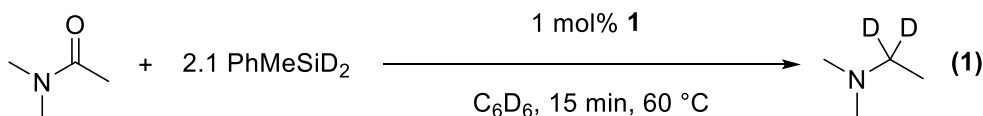
Table 5. (continued)

24	80	35
48	88.5	37.5
96	93.5	40

^a Yield and conversion calculated by ¹H NMR

In an experiment to see if the order of addition of amide and silane has any impact on the reaction, there was no difference with the reaction when either amide or silane was added to the catalyst first. When the catalyst is added to N,N-dimethylbenzamide in stoichiometric quantity, the amide exhibits some changes in ¹H NMR shifts. The methyl peaks on the amide nitrogen shift from 2.75 + 2.31 ppm in benzene-*d*₆ to 2.56 + 2.17 ppm. (Coupling constants change from 176 Hz to 156 Hz). The catalyst is not entirely soluble in benzene until the addition of the silane, but similar observations were made in deuterated bromobenzene. (2.82 + 2.55 ppm to 2.90 + 2.71 ppm, 108 Hz to 75 Hz).

Other reductants were tested with amides and **1** in place of hydrosilanes. When HBPin was used in place of PhSiH₃, no amines were identified in solution via ¹H NMR in benzene-*d*₆ or GC-MS after reactions in which the reaction was heated up to 120 °C. Hydrogen gas was also tested as a reductant, and under 1 atm H₂, no amines were observed but the cyclooctadiene on the catalyst was hydrogenated to form cyclooctane as observed by ¹H NMR. The catalyst is effective for alkene hydrogenation with hydrogen, as evidenced with hydrogenation of olefin containing amides.



To determine the origin of the protons which reduce the amide, an experiment with deuterated phenylmethylsilane and N,N-dimethylacetamide was performed (Eq. 1). The results indicate that the protons from the reduction come directly from the silane, as evidenced by the absence of the CH₂ peak of N,N-dimethylacetamide in ¹H NMR after the completion of the reduction.

Investigation into the mechanism of the reaction led us to attempt to determine the active species present during catalysis. Addition of PhSiH₃ or Ph₂SiH₂ to **1** in CD₂Cl₂ or C₆D₅Br led to rapid decomposition of the catalyst at room temperature. Other attempts were made toward synthesizing the neutral Rh silyl followed by addition of a halide abstracting agent by preparing the analog to a previously reported Xantphos Rh silyl compound.²¹ When NaBAR^F or AgBF₄ was added to XantphosRh(Cl)(H)(SiHPh₂) in either CD₂Cl₂ or C₆D₅Br, the product rapidly decomposed. We concluded that the active species was too reactive to isolate.

Conclusions

In summary, we utilize XantphosRh(cod)BAR^F as an effective catalyst for reduction of both secondary and tertiary amides. This catalyst has modest functional group tolerance, and allows for the reductions to occur at mild temperatures in short times with good yield. Conditions must be modified for successful reactions depending

on substrate, due to reactivity of the catalyst and its efficacy as an olefin-hydrogenation catalyst.

Mechanistic study of the reaction confirms that the protons used to reduce the amide come from the silane, not from elsewhere, but the active species of catalyst is still unknown. Attempts to isolate potential active species were unsuccessful due to the reactivity of the catalyst. Finally, disproportionation of phenylsilane was investigated and it was determined that it is likely the source of hydrogen for olefin hydrogenations.

Experimental

Synthesis of XantphosRh(cod)BAr^F (1) Xantphos (0.100 g, 0.173 mmol), [RhCl(cod)]₂ (0.046 g, 0.086 mmol) and NaBAr^F (0.150 g, 0.173 mmol) was suspended in CH₂Cl₂ (15 mL). It was allowed to stir at room temperature for 2 h. NaCl was removed by filtration and the solvent was removed under vacuum to afford **1** as an orange-red crystalline powder (0.278 g, 0.168 mmol, 97.3%)

¹H (400.39 MHz, CD₂Cl₂, 298 K): δ 7.72 (m, 8H, BAr^F₄), 7.70 (s, 2H), 7.56 (s, 4H, BAr^F₄), 7.27 (m, 6H, aryl), 7.14 (m, 16H, aryl), 7.03 (m, 2H, aryl), 4.42 (m, 4H, cod), 2.23 (m, 4H, cod), 2.01 (m, 4H, cod), 1.84 (s, 6H, CH₃). ³¹P {¹H} NMR (162.08 MHz, CD₂Cl₂, 298K): δ 8.43 (d, J_{Rh-P} 136 Hz)

Anal. Calcd. for C₇₉H₅₆BF₂₄OP₂Rh: C, 57.40; H, 3.42 Found: C, 57.84; H, 3.24.

General procedure for amide reduction.

Amide (0.1 mmol), phenylsilane (0.21 mmol) and XantphosRh(cod)BAr^F (0.001 mmol) was dissolved in benzene (5.0 mL) in a scintillation vial and either left at room temperature or heated to 60 °C while stirring for the time as described in Table 3. After the time elapsed, the solution was filtered through a celite plug to remove excess Rh. Ethereal HCl was added to precipitate out the amine salt, which was washed with ether and dried under vacuum.

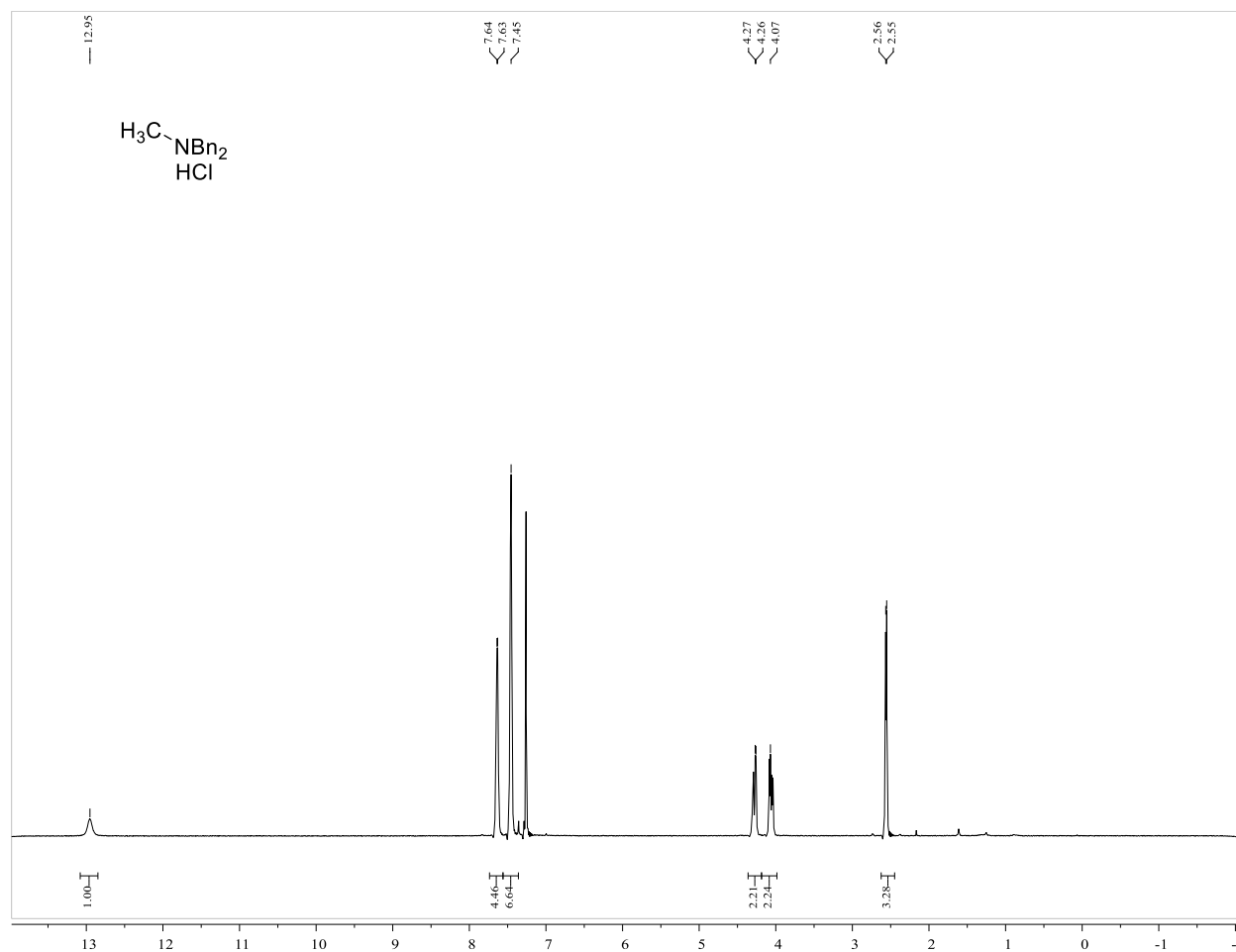
References

- (1) Ricci, A. *Modern Amination Methods*; Wiley: New York, 2007.
- (2) Andersson, P. G.; Schink, H. E.; Österlund, K. *J. Org. Chem.* **1998**, *63* (22), 8067–8070.
- (3) Gill, C. D.; Greenhalgh, D. A.; Simpkins, N. S. *Tetrahedron* **2003**, *59* (46), 9213–9230.
- (4) Giles, M. E.; Thomson, C.; Eyley, S. C.; Cole, A. J.; Goodwin, C. J.; Hurved, P. A.; Morlin, A. J. G.; Tornos, J.; Atkinson, S.; Just, C.; Dean, J. C.; Singleton, J. T.; Longton, A. J.; Woodland, I.; Teasdale, A.; Gregertsen, B.; Else, H.; Athwal, M. S.; Tatterton, S.; Knott, J. M.; Thompson, N.; Smith, S. J. *Org. Process Res. Dev.* **2004**, *8* (4), 628–642.
- (5) Magano, J.; Dunetz, J. R. *Org. Process Res. Dev.* **2012**, *16* (6), 1156–1184.
- (6) Kuwano, R.; Takahashi, M.; Ito, Y. *Tetrahedron Lett.* **1998**, *39* (9), 1017–1020.

- (7) Park, S.; Brookhart, M. *J. Am. Chem. Soc.* **2012**, *134* (1), 640–653.
- (8) Cheng, C.; Brookhart, M. *J. Am. Chem. Soc.* **2012**, *134* (28), 11304–11307.
- (9) Hanada, S.; Tsutsumi, E.; Motoyama, Y.; Nagashima, H. *J. Am. Chem. Soc.* **2009**, *131* (41), 15032–15040.
- (10) Laval, S.; Dayoub, W.; Pehlivan, L.; Méta y, E.; Favre-Réguillon, A.; Delbrayelle, D.; Mignani, G.; Lemaire, M. *Tetrahedron Lett.* **2011**, *52* (32), 4072–4075.
- (11) Zhuo, S.; Junge, K.; Addis, D.; Das, S.; Beller, M. *Angew. Chem. Int. Ed.* **2009**, *48* (50), 9507–9510.
- (12) Pisiewicz, S.; Junge, K.; Beller, M. *Eur. J. Inorg. Chem.* **2014**, No. 14, 2345–2349.
- (13) Zhang, T.; Zhang, Y.; Zhang, W.; Luo, M. *Adv. Synth. Catal.* **2013**, *355* (14–15), 2775–2780.
- (14) Li, Y.; Molina De La Torre, J. A.; Grabow, K.; Bentrup, U.; Junge, K.; Zhou, S.; Brückner, A.; Beller, M. *Angew. Chem. Int. Ed.* **2013**, *52* (44), 11577–11580.
- (15) Kranenburg, M.; van der Burgt, Y. E. M.; Kamer, P. C. J.; van Leeuwen, P. W. N. M.; Goubitz, K.; Fraanje, J. *Organometallics* **1995**, *14* (6), 3081–3089.
- (16) Jiang, Y. Y.; Yu, H. Z.; Fu, Y. *Organometallics* **2013**, *32* (3), 926–936.
- (17) Sandee, A. J.; Van Der Veen, L. A.; Reek, J. N. H.; Kamer, P. C. J.; Lutz, M.; Spek, A. L.; Van Leeuwen, P. W. N. M. *Angew. Chem. Int. Ed.* **1999**, *38* (21), 3231–3235.
- (18) Williams, G. L.; Parks, C. M.; Smith, C. R.; Adams, H.; Haynes, A.; Meijer, A. J.

- H. M.; Sunley, G. J.; Gaemers, S. *Organometallics* **2011**, *30* (22), 6166–6179.
- (19) Dallanegra, R.; Chaplin, A. B.; Weller, A. S. *Organometallics* **2012**, *31* (7), 2720–2728.
- (20) Pawley, R. J.; Moxham, G. L.; Dallanegra, R.; Chaplin, A. B.; Brayshaw, S. K.; Weller, A. S.; Willis, M. C. *Organometallics* **2010**, *29* (7), 1717–1728.
- (21) Esteruelas, M. A.; Oliván, M.; Vélez, A. *Inorg. Chem.* **2013**, *52* (20), 12108–12119.
- (22) Esteruelas, M. A.; Oliván, M.; Vélez, A. *Inorg. Chem.* **2013**, *52*, 5339–5349.
- (23) van Haaren, R. J.; Zuidema, E.; Fraanje, J.; Goubitz, K.; Kamer, P.; van Leeuwen, P. W.; van Strijdonck, G. *C.R. Chim.* **2002**, *5*, 431–440.
- (24) Rosenberg, L.; Davis, C. W.; Yao, J. *J. Am. Chem. Soc.* **2001**, *123* (21), 5120–5121.
- (25) Rosenberg, L. *Macromol. Symp.* **2003**, *196*, 347–353.

Supporting Information

Figure S7. ^1H NMR Spectra. Table 3 - Entry 1

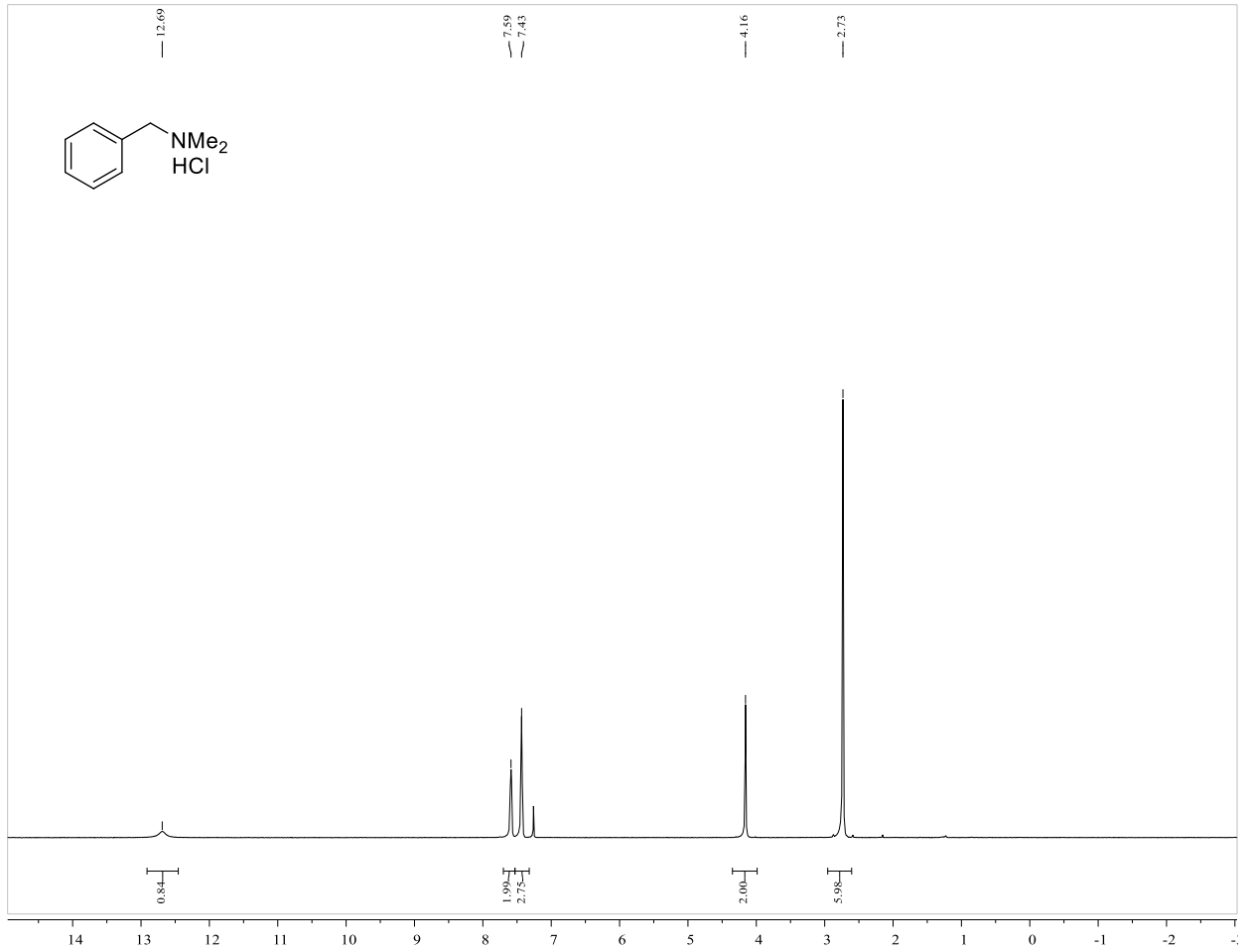


Figure S2. ^1H NMR Spectra. Table 3 - Entry 2

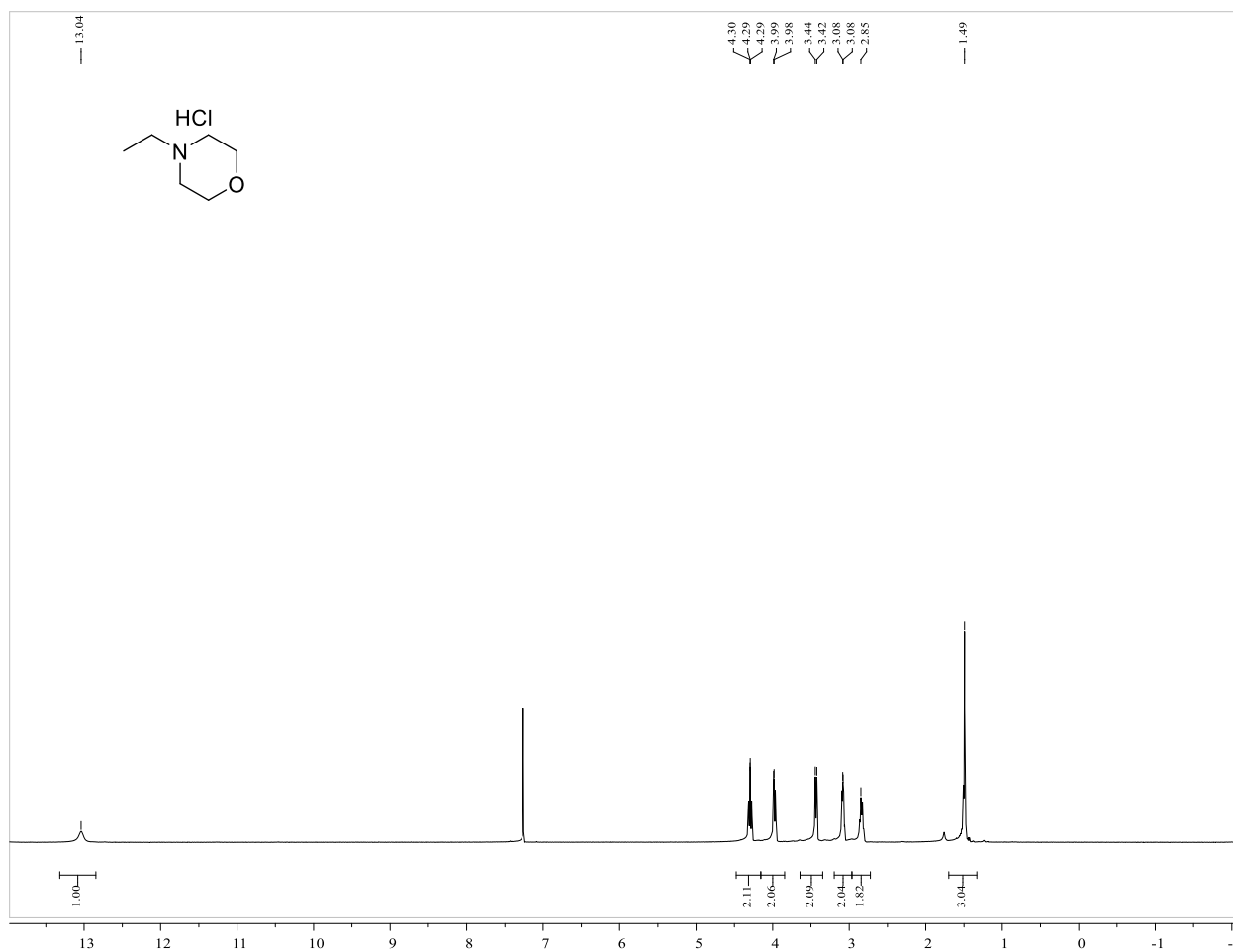


Figure S3. ¹H NMR Spectra. Table 3 - Entry 3

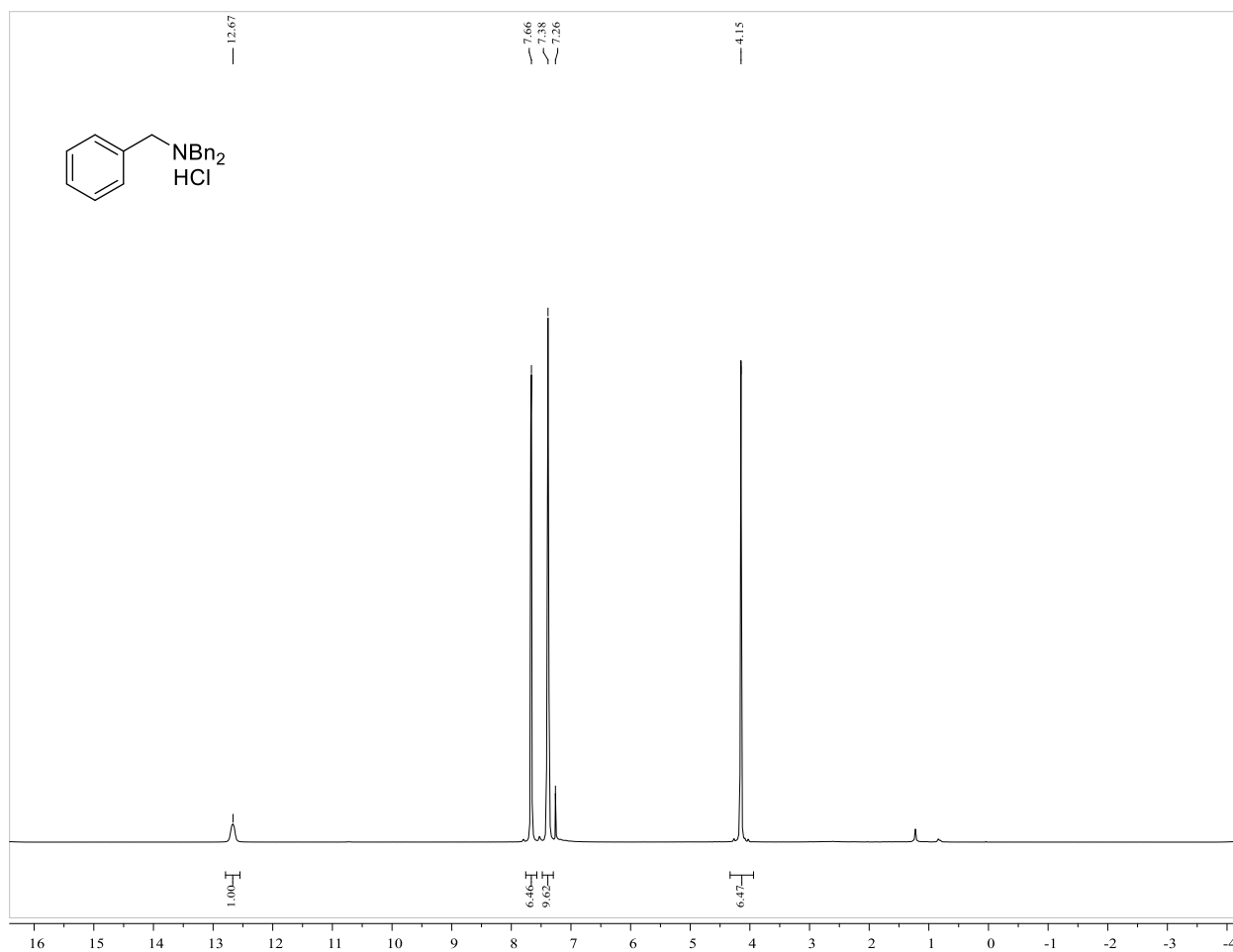


Figure S4. ^1H NMR Spectra. Table 3 - Entry 4

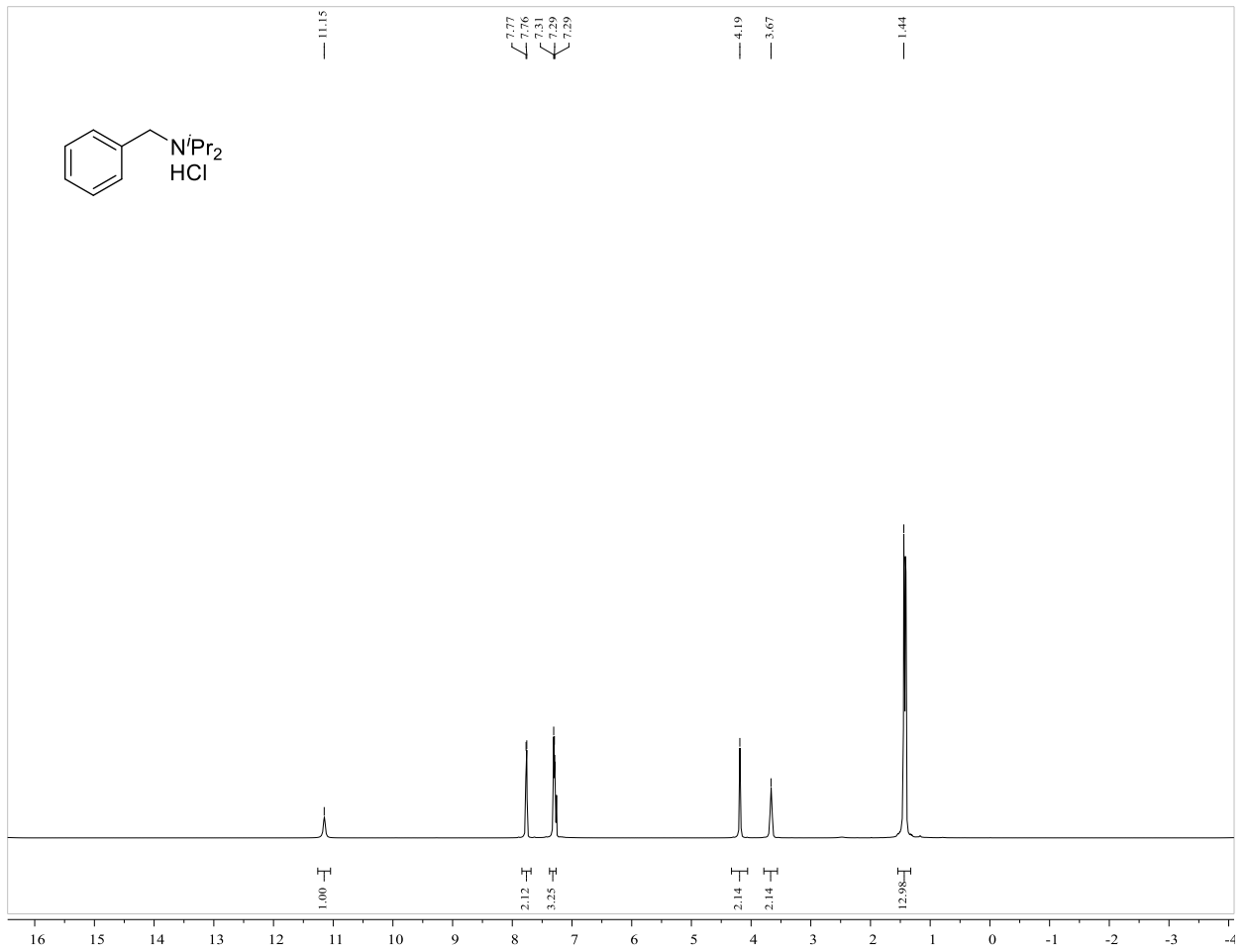


Figure S5. ^1H NMR Spectra. Table 3 - Entry 5

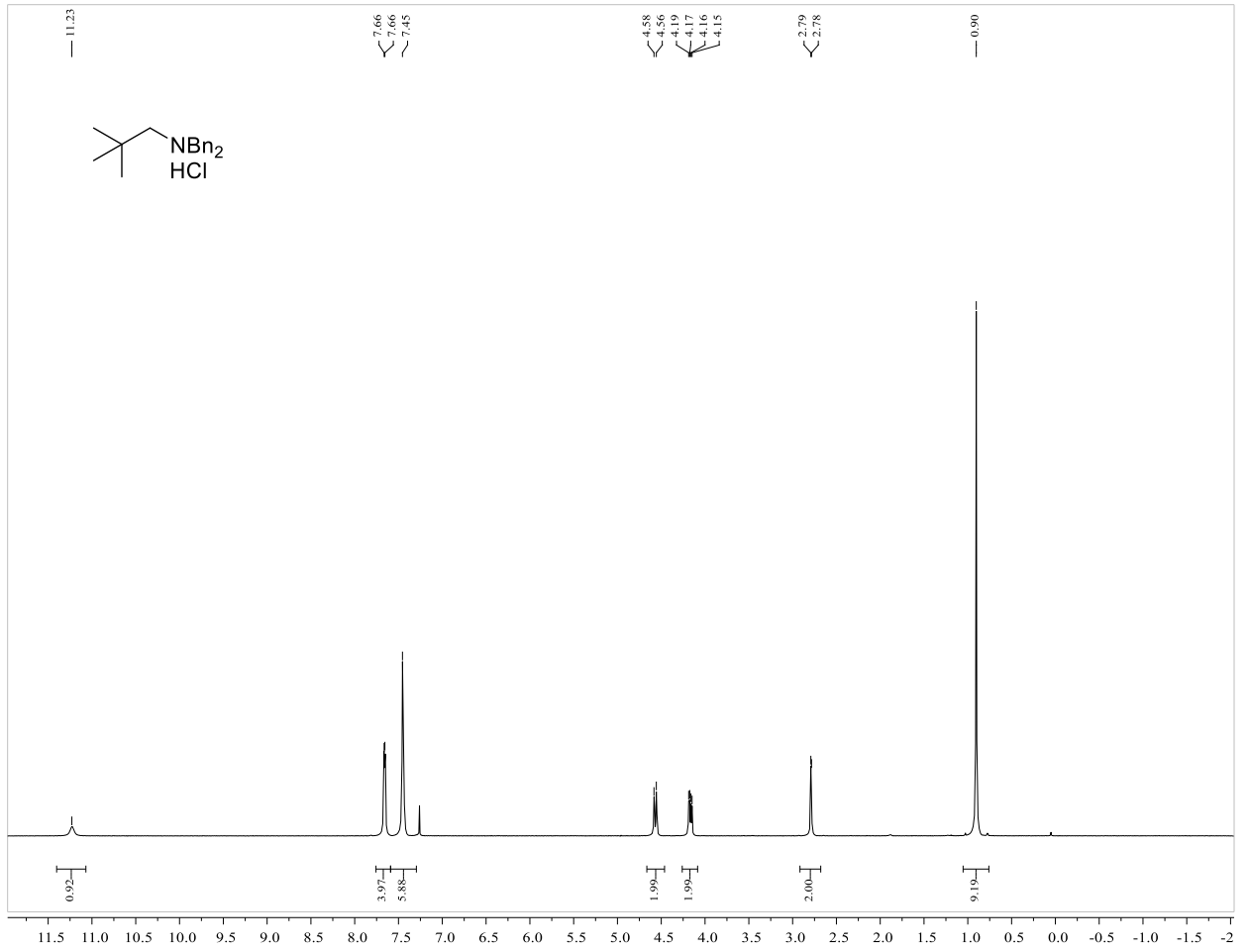


Figure S6. ^1H NMR Spectra. Table 3 - Entry 6

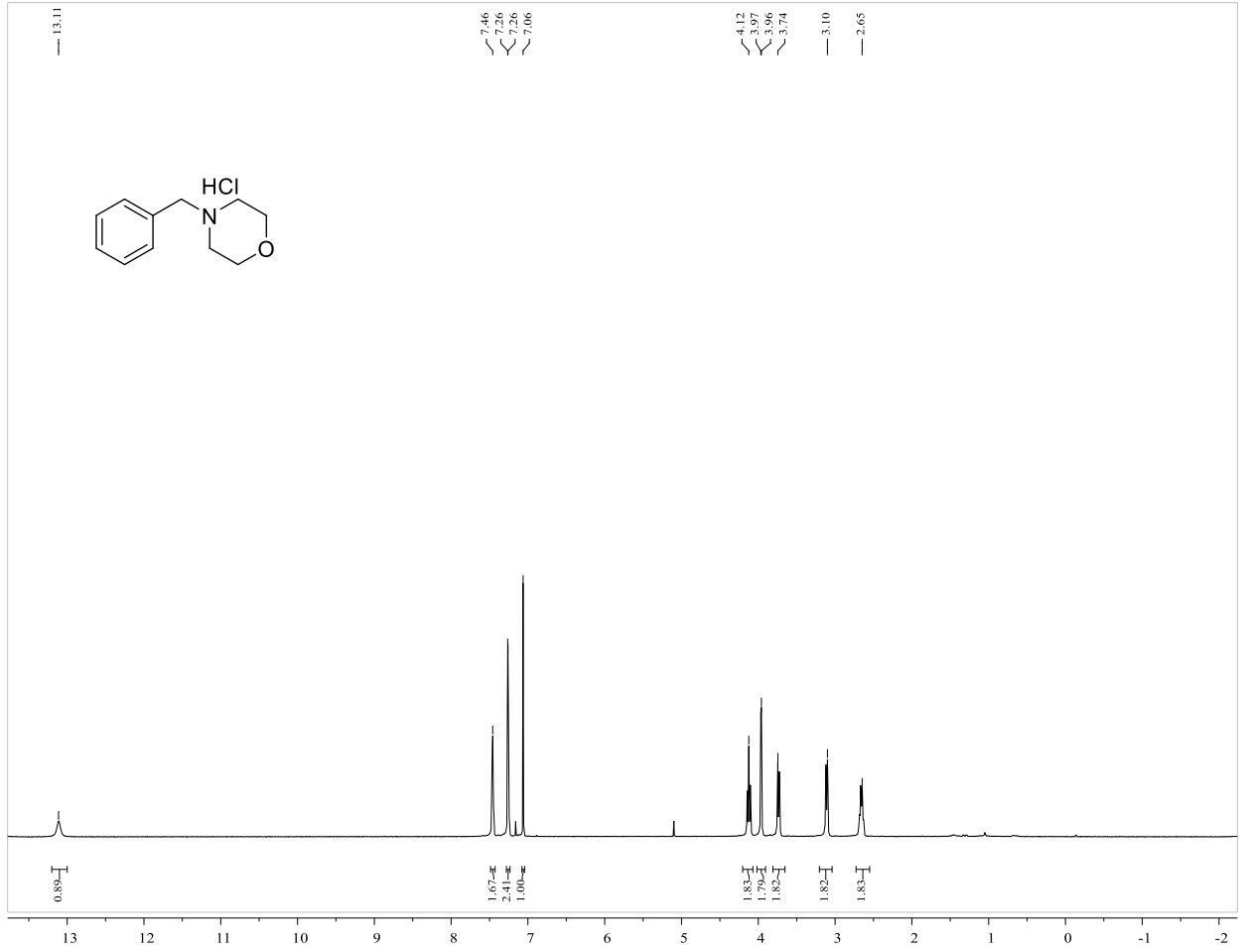


Figure S8. ¹H NMR Spectra. Table 3 - Entry 8

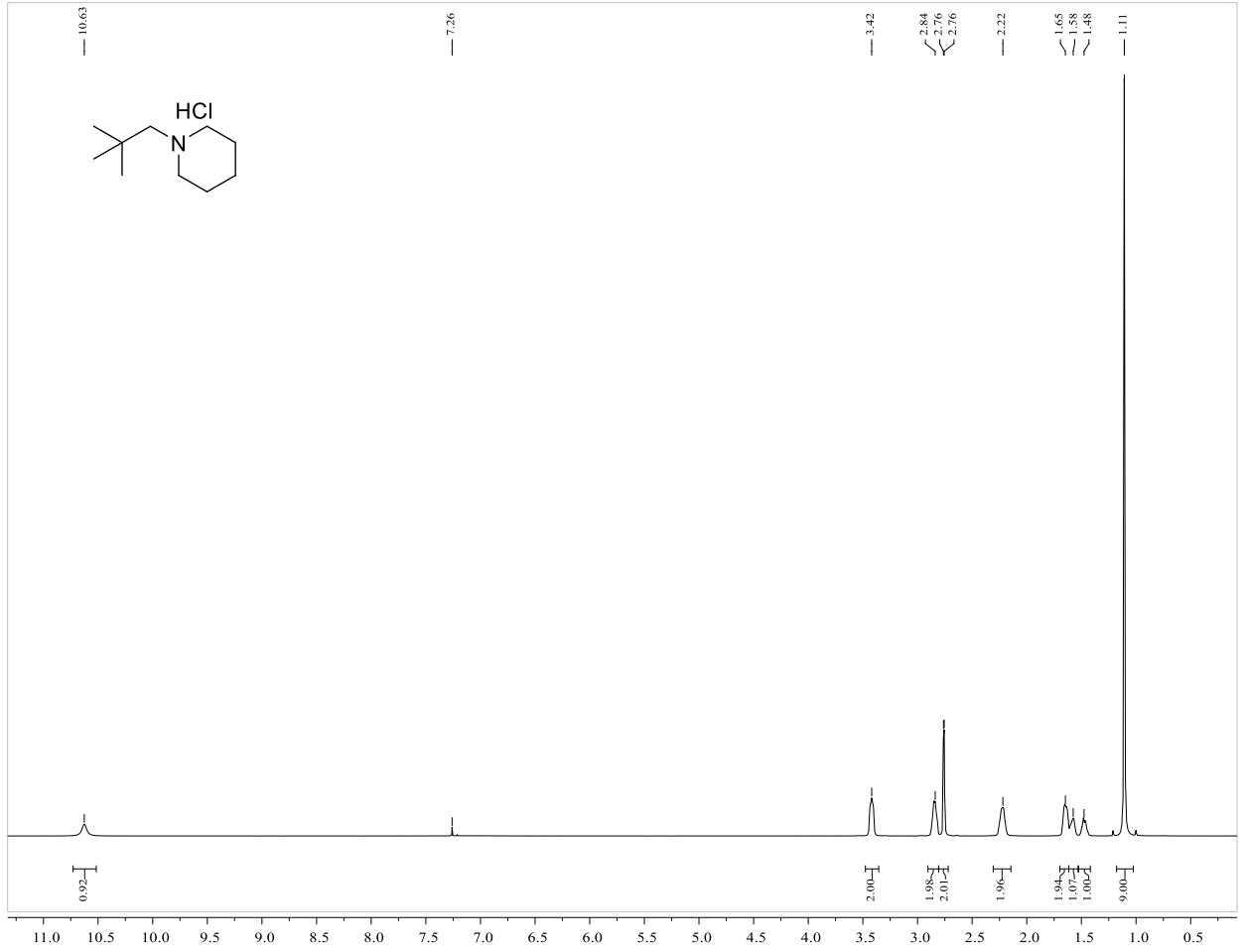


Figure S9. ¹H NMR Spectra. Table 3 - Entry 9

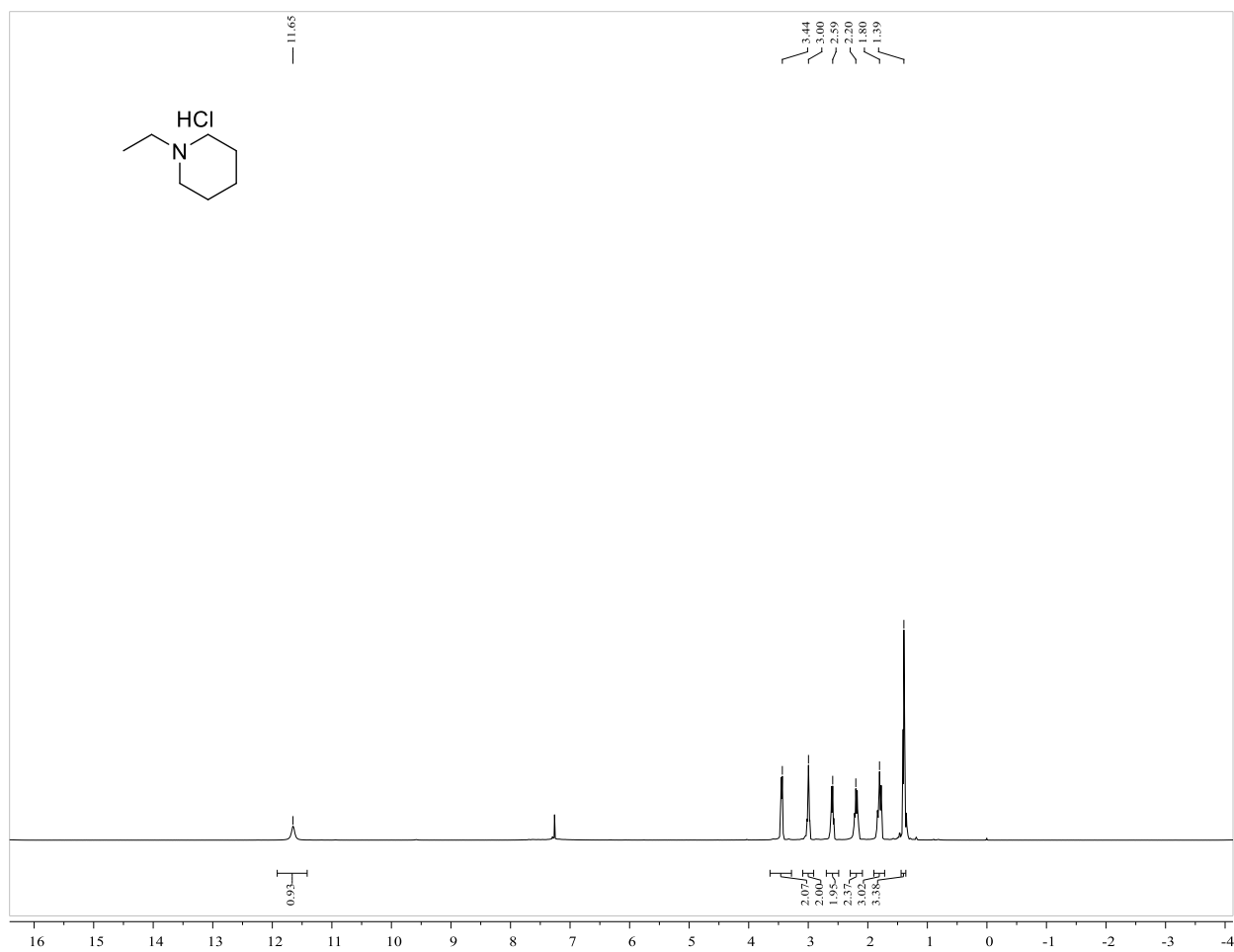


Figure S10. ^1H NMR Spectra. Table 3 - Entry 10

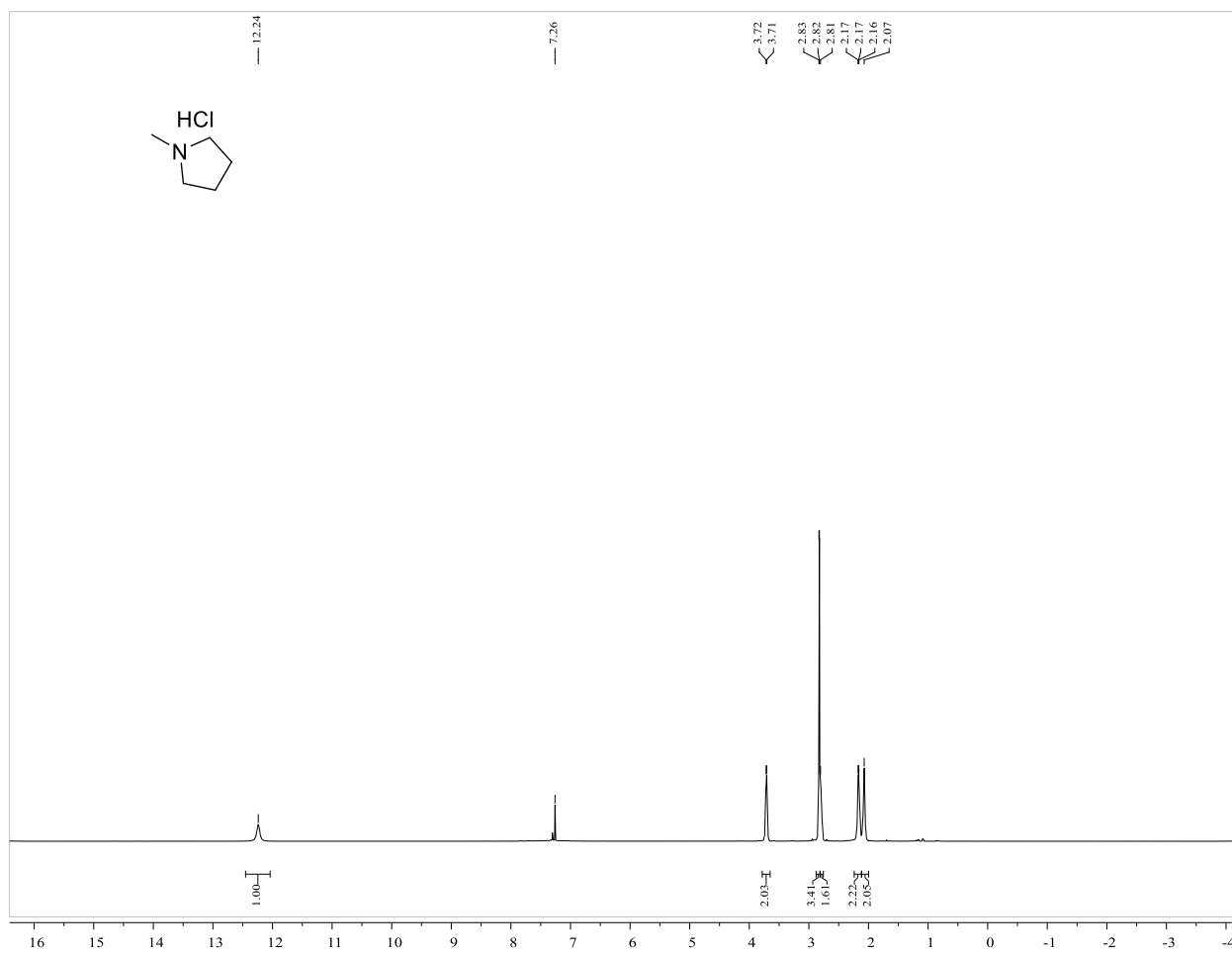


Figure S11. ¹H NMR Spectra. Table 3 - Entry 11

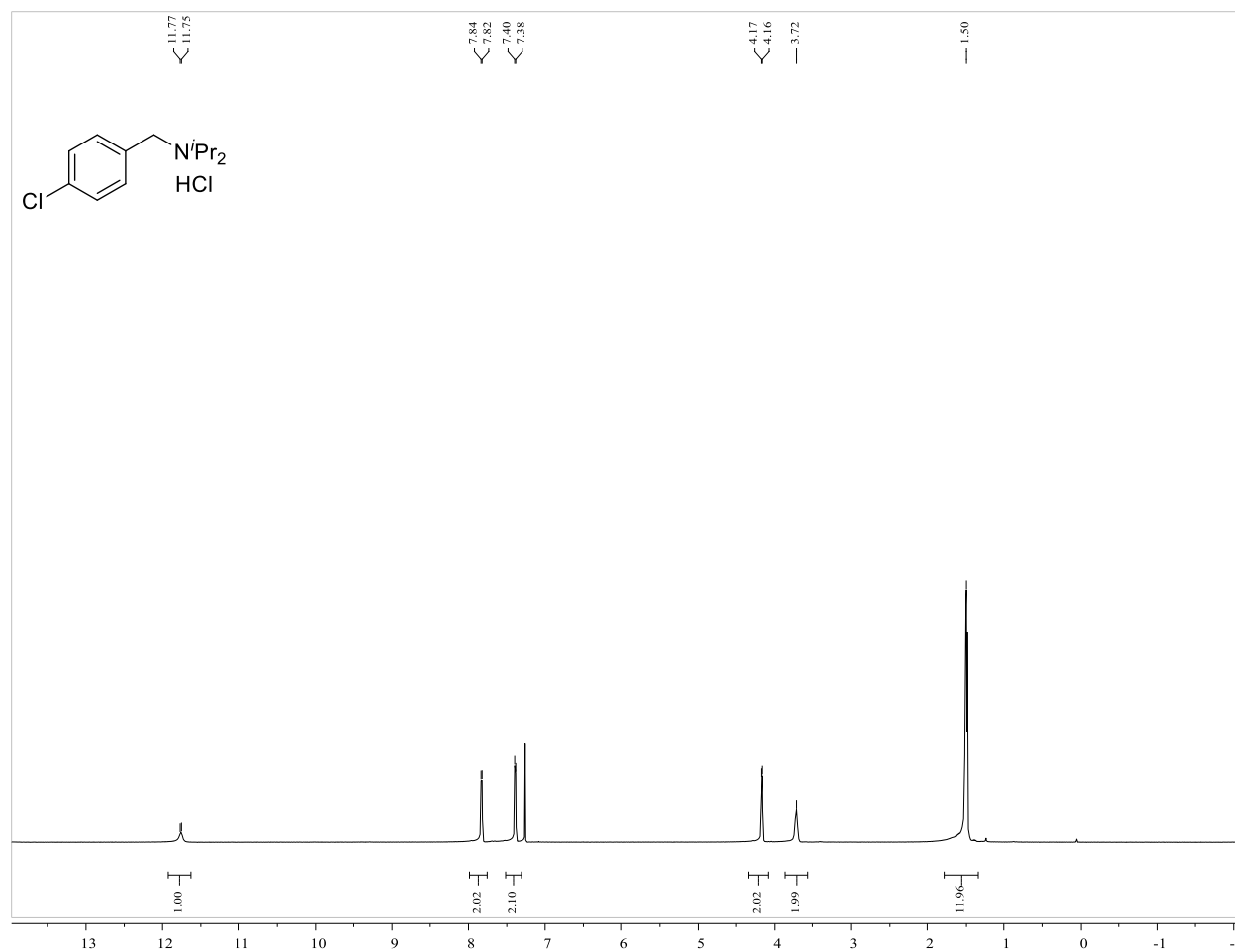


Figure S12. ^1H NMR Spectra. Table 3 - Entry 12

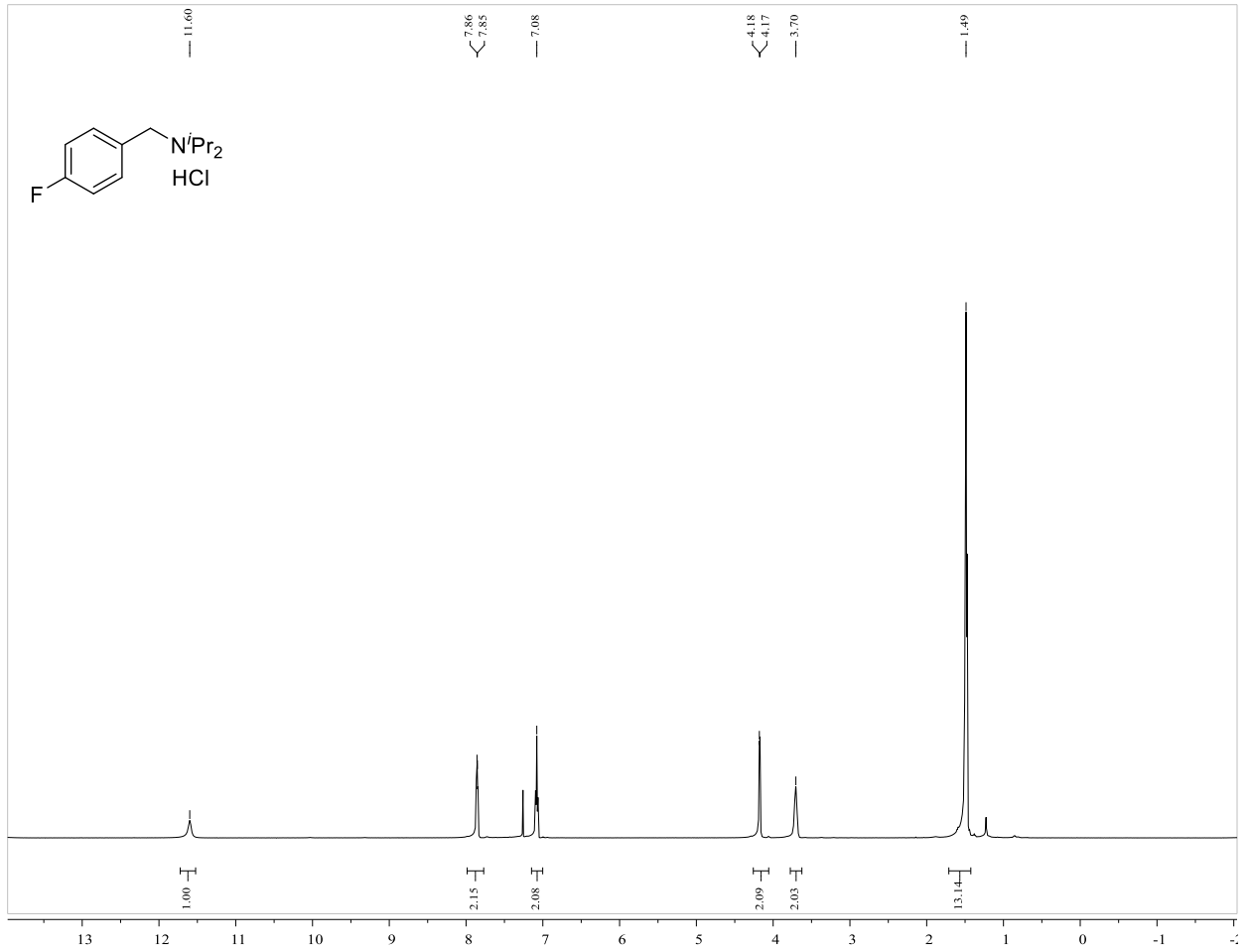


Figure S13. ¹H NMR Spectra. Table 3 - Entry 13

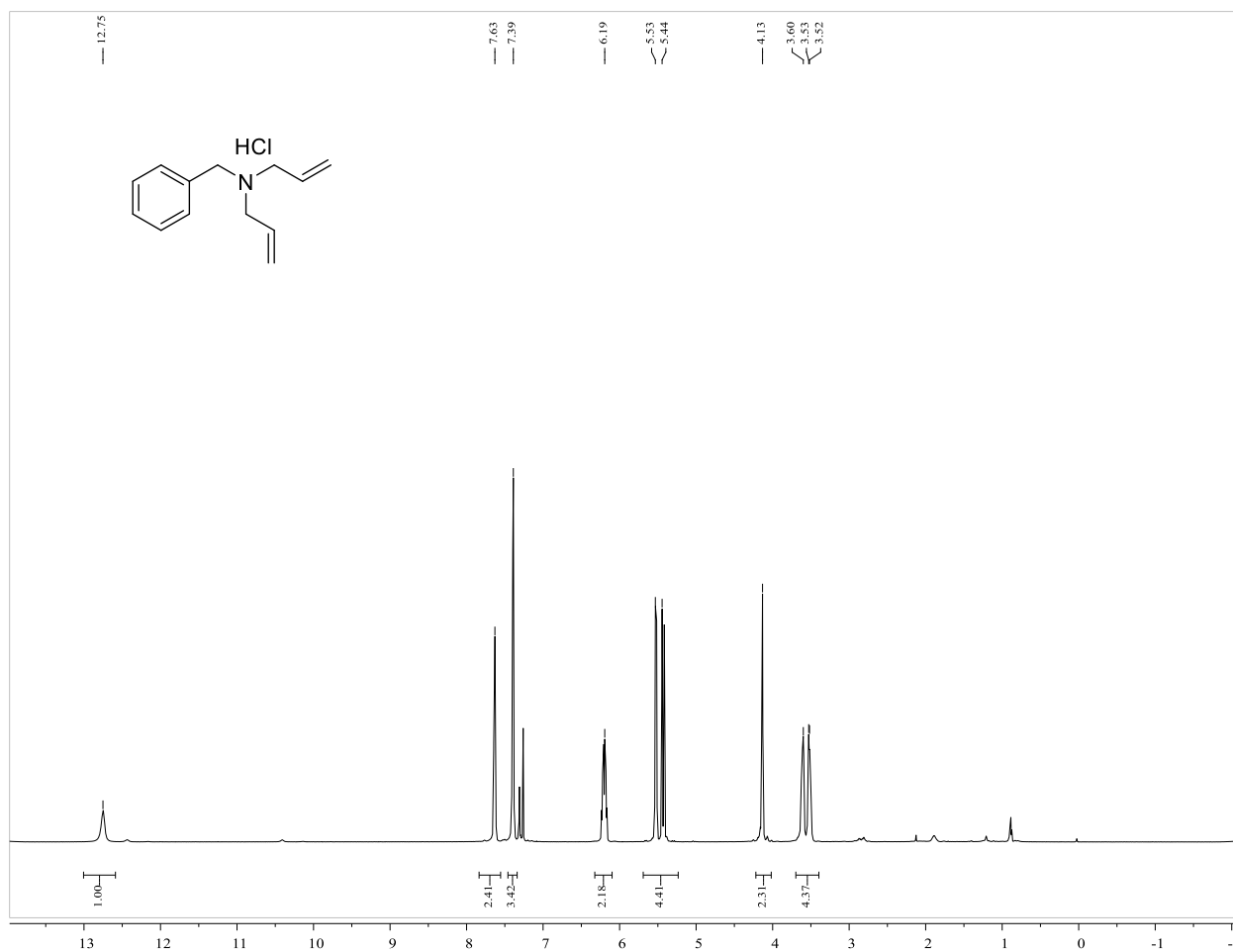


Figure S14. ¹H NMR Spectra. Table 3 - Entry 14

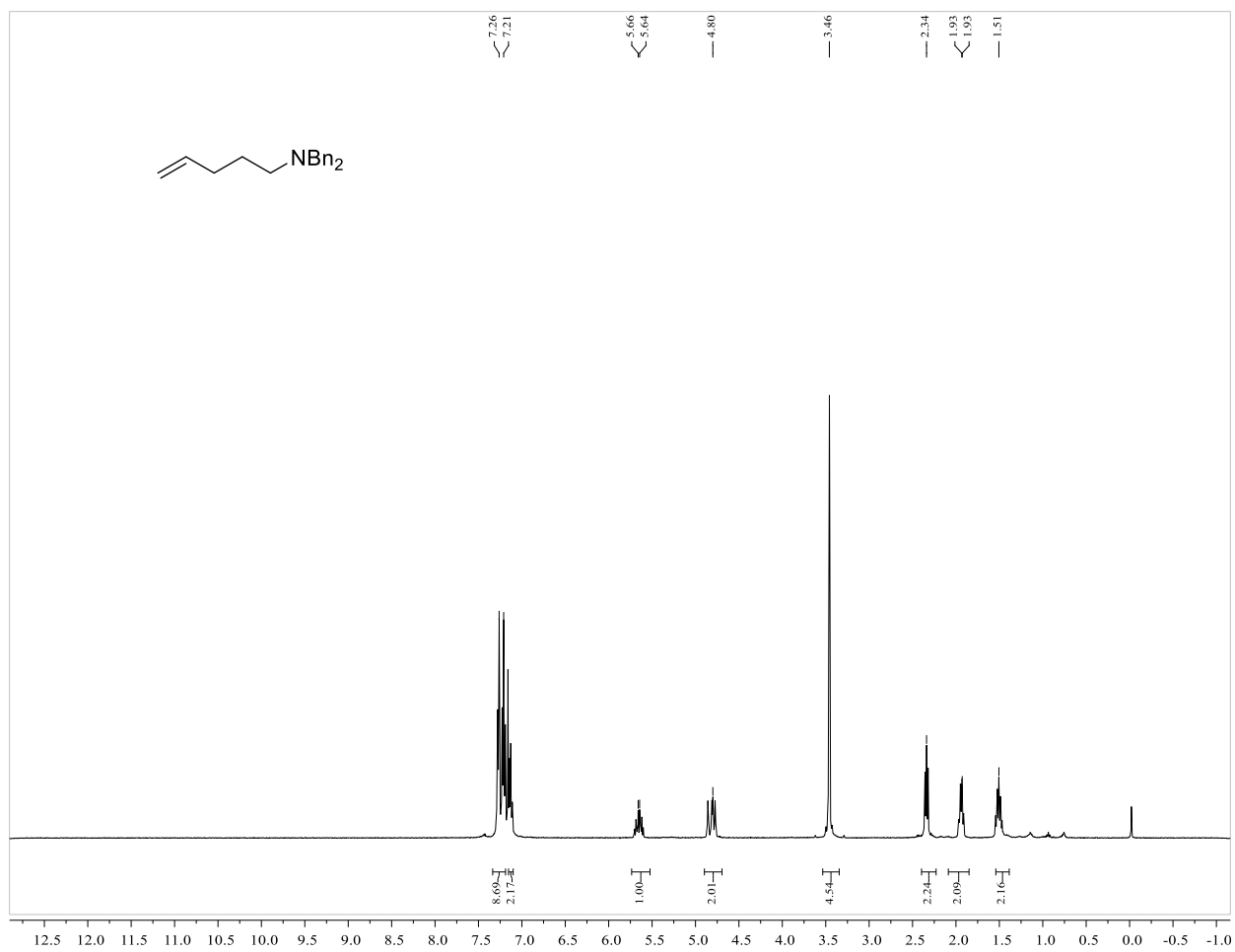


Figure S15. ¹H NMR Spectra. Table 3 - Entry 15

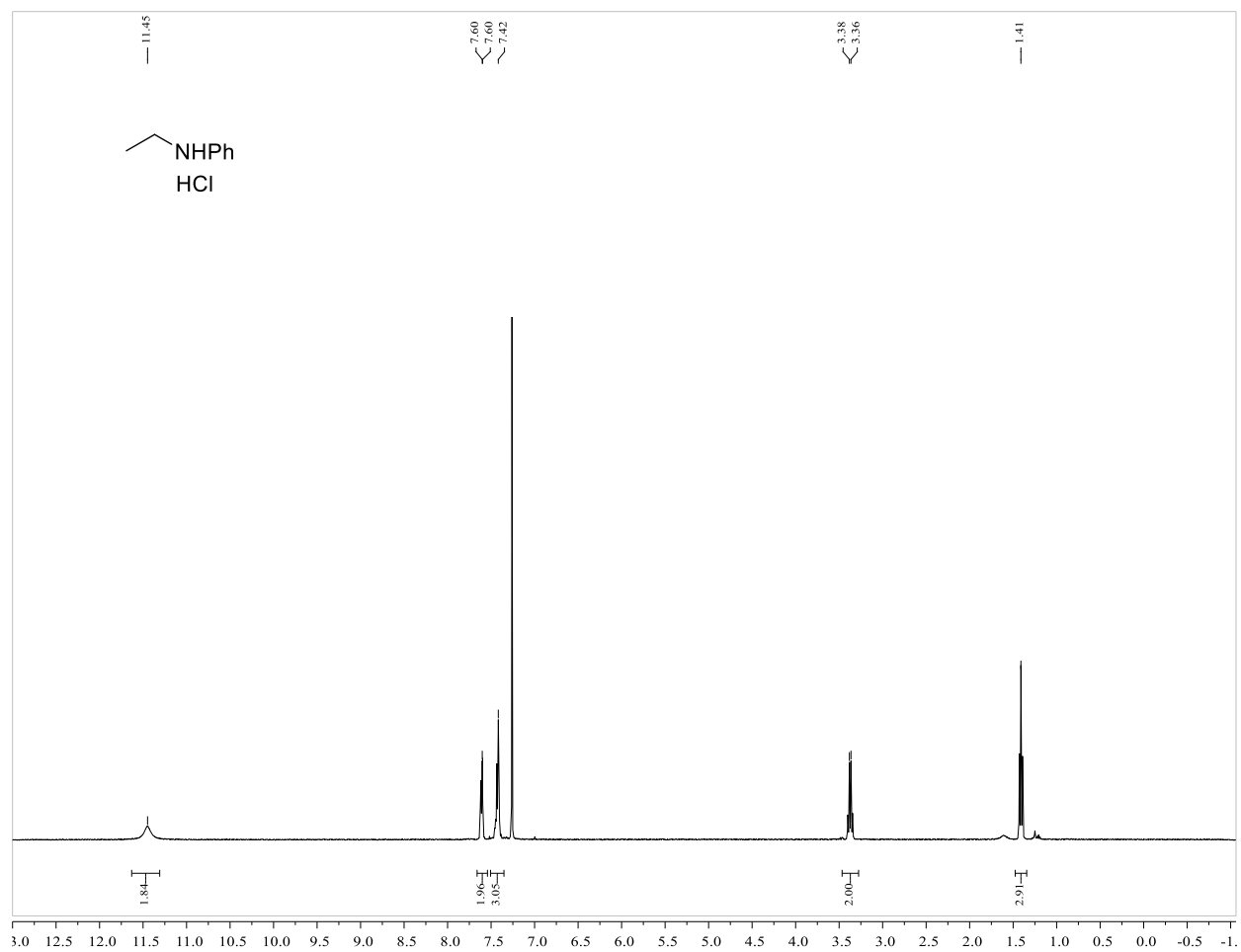


Figure S16. ^1H NMR Spectra. Table 4 - Entry 16

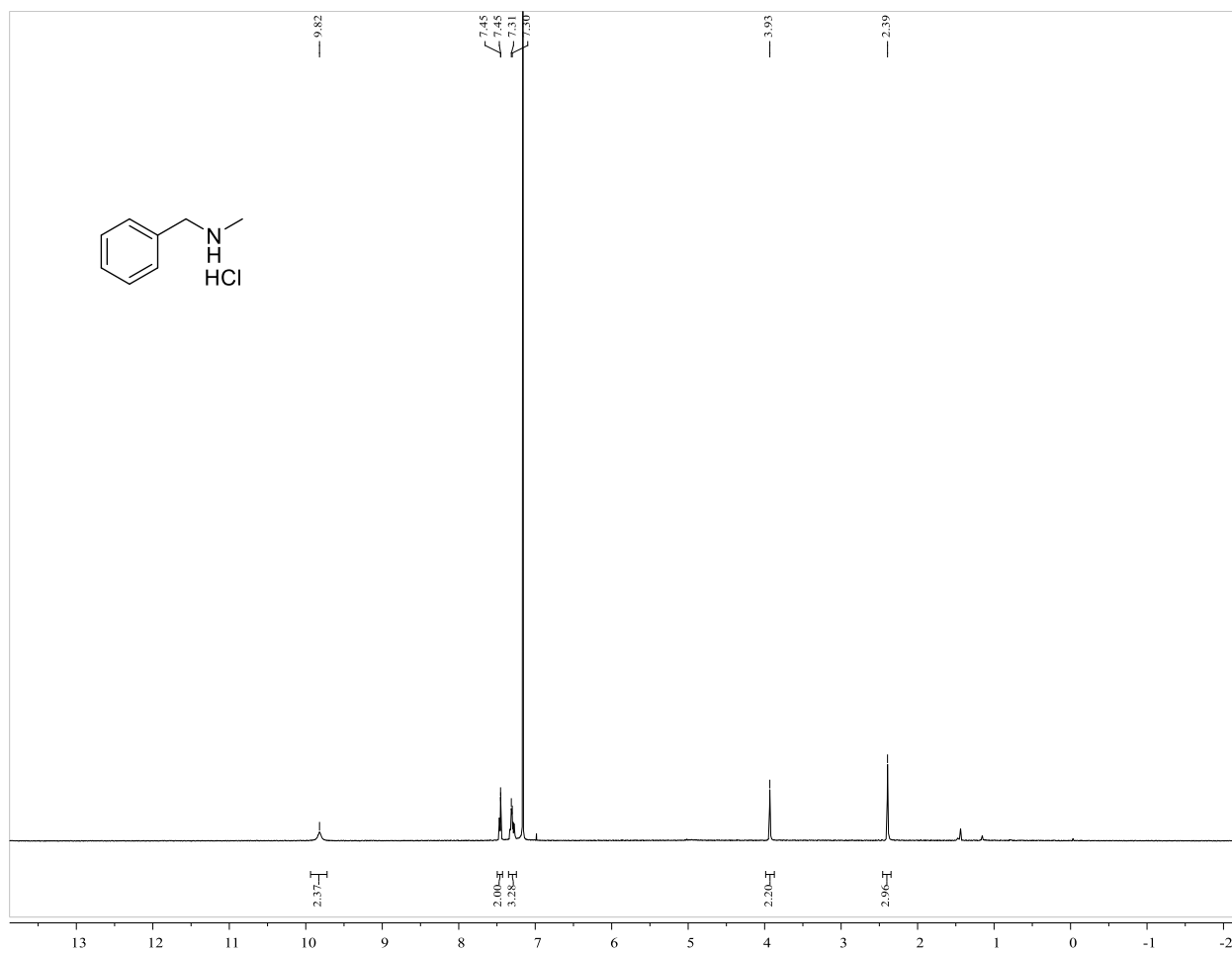


Figure S17. ¹H NMR Spectra. Table 4 - Entry 17

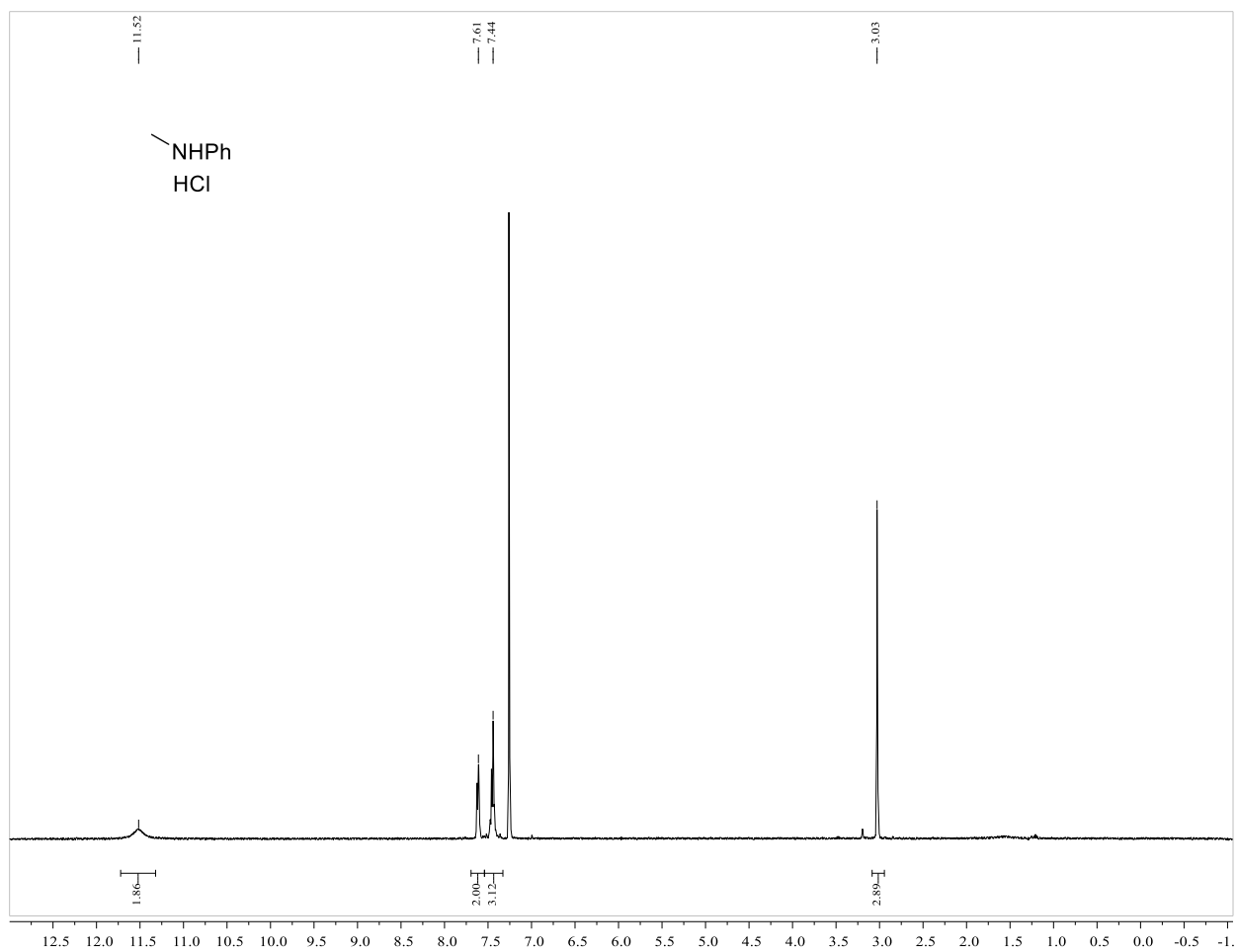


Figure S18. ^1H NMR Spectra. Table 4 - Entry 18

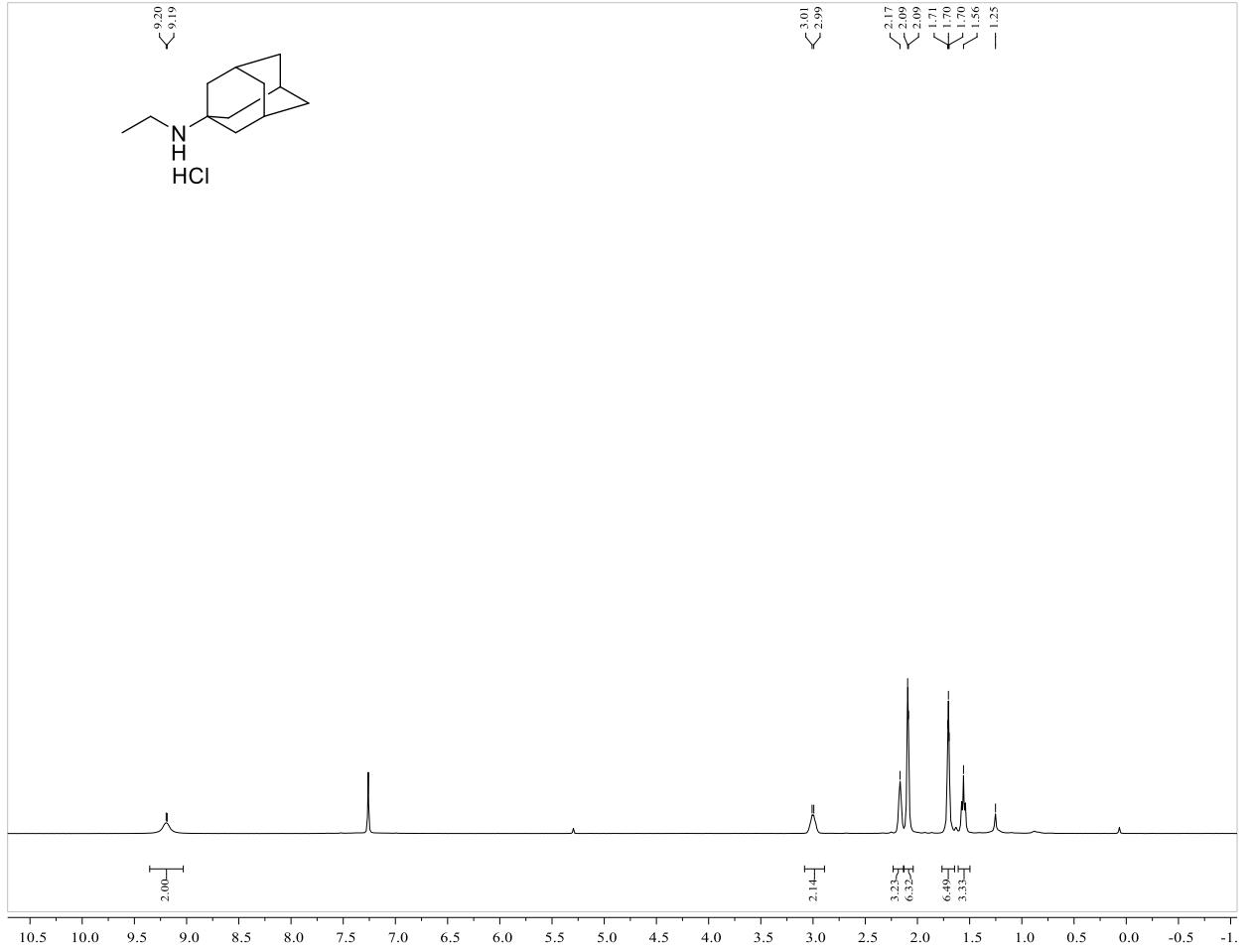


Figure S19. ^1H NMR Spectra. Table 4 - Entry 19

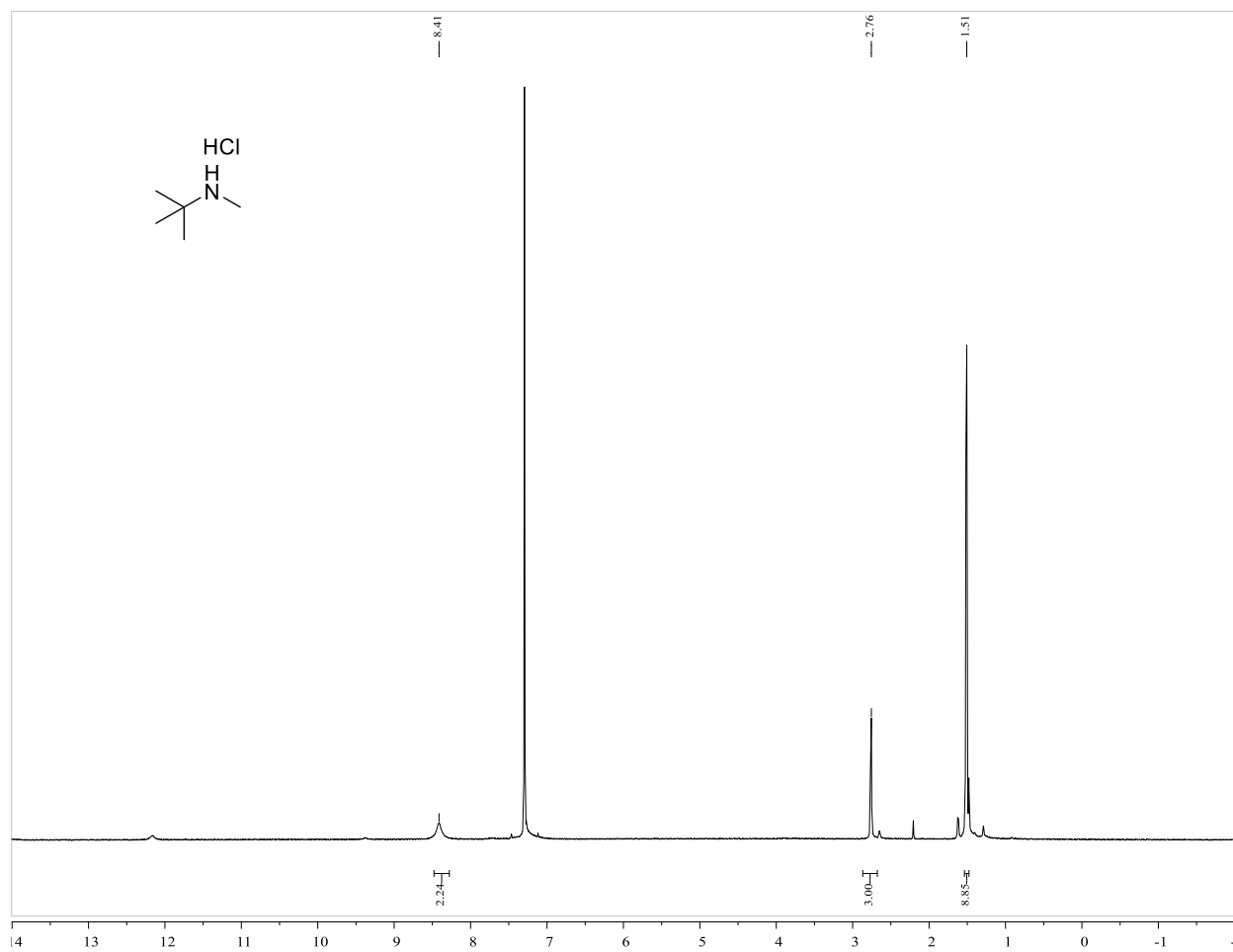


Figure S20. ^1H NMR Spectra. Table 4 - Entry 20

CHAPTER 5. CONCLUSION

Studies were performed on a series of catalytic reactions using both conventional synthetic strategies and strategies based on the operation of our automated synthesis platform. New catalysts were identified for Henkel-type reactions, amide reductions and hydrogenolysis reactions. New methods were developed for studying the kinetics of catalytic oxidation reactions and enyne metathesis reactions.

Synthesis of 2,5-FDCA was achieved in high yield from potassium furoate catalyzed by copper(I) iodide under high pressures of carbon dioxide. Yield and selectivity have increased from previously identified Zn- and Cd- based catalysts. Carbon dioxide plays a strong role in the catalytic cycle, although the overall mechanism is not known. Other dicarboxylates can be accessed from other potassium carboxylate precursors, but non-heteroaromatic carboxylates require higher temperatures than that of furoate. These reactions can possibly provide new opportunities for large scale synthesis of polymer precursors.

The strengths and weaknesses of using an automated synthesis platform were realized as several uniquely different experiments were developed on the instrument. First, the reaction of the oxidation of cyclohexane was studied over time, acquiring information to study the kinetics of the reaction as catalyzed by Ni, Fe and Co complexes. Secondly, heterogeneous catalysts were synthesized in usable scale quantities by iterative addition of pre-catalyst solution. The synthesis was entirely automated, and the resulting products were used as catalysts for the hydrogenolysis of lignin model

compounds for the eventual goal bio-mass upgrading. Finally, the stainless steel high-pressure reactors were used to optimize the synthesis of butadiene analogs.

Finally, a series of secondary and tertiary amines were synthesized from their respective amides in a hydrosilane induced reduction catalyzed by XantphosRh(cod)BAR^F. The amines were mostly synthesized in high yield with modest functional group tolerance at mild temperatures in short times. The catalyst was found to disproportionate phenylsilane rapidly producing hydrogen gas as well as other aryl silanes.